V CHAPTER : ELECTRONIC STRUCTURE OF TRANSITION METAL-HYDRIDES

V.1 PRELIMINARY REMARKS

For years the electronic structure of metal-hydride systems has been discussed within one-electron band structure theories. This type of theory works well for the hydrides of transition metals such as V, Nb, Ta and Pd. These metallic hydrides are discussed in the present chapter using the simple approach of the **tight-binding approximation**. This is by no means the best band structure calculation technique but it provides a physically transparent, though semi-quantitative picture of the parameters that determine the electronic structure of transition metals. It is also often used as an interpolation scheme between accurately calculated energies at special **k**-points in the Brillouin zone.

However, the discovery of metal-hydrides with switchable optical properties such as YH_x and LaH_x demonstrated vividly that these one-electron theories were not adequate and that correlation effects had to be taken into account. The electronic structure of these materials shall be discussed in Chapter VI together with electron correlation effects in the negative H^- ion. Finally, the discovery of rare-earth-free switchable metal-hydrides such Mg_2NiH_x and new storage compounds such as $NaAlH_4$ revived the interest in the electronic structure of complex metal-hydrides. These are discussed in Chapter VII.

V.2 ONE-ELECTRON BAND STRUCTURES

In Fig. V.1 we show the band structure of Pd that is a sort of archetypal FCC metal-hydride forming metal. Like all the transition metals with a FCC crystal structure Pd exhibits along the ΓX direction in the Brillouin zone two types of bands i) a broad s-p band and a relatively narrow set (5) of d-bands.

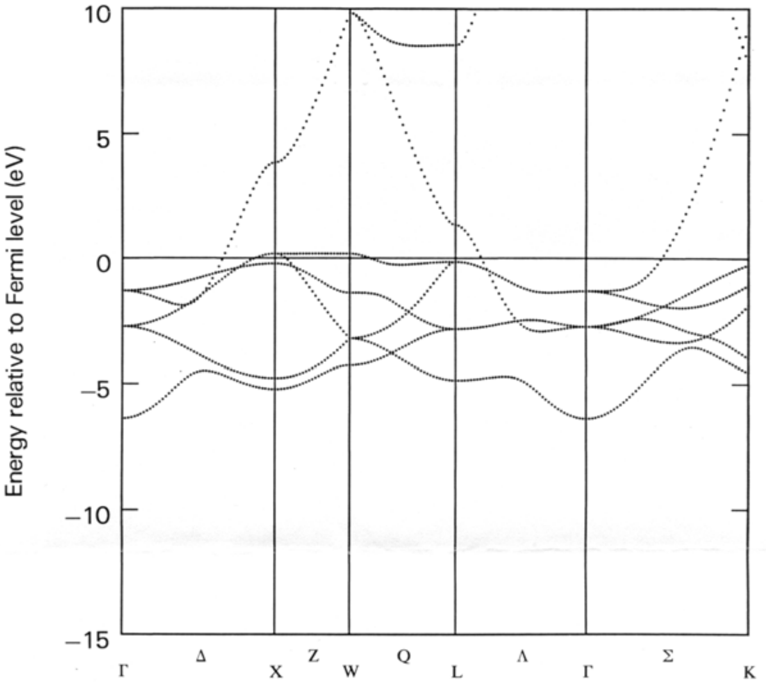

Fig. V.1: Band structure of Pd. The meaning of the symbols is explained below in the left panel depicting the Brillouin zone (from Moruzzi[1]). The Fermi surface is shown in the right panel. The flat d-bands give rise to the complex purple structure[2]. The s-p band determines the green electron sheet of the Fermi surface. The little yellow ellipsoids are holes at the top of the d-band near point X.

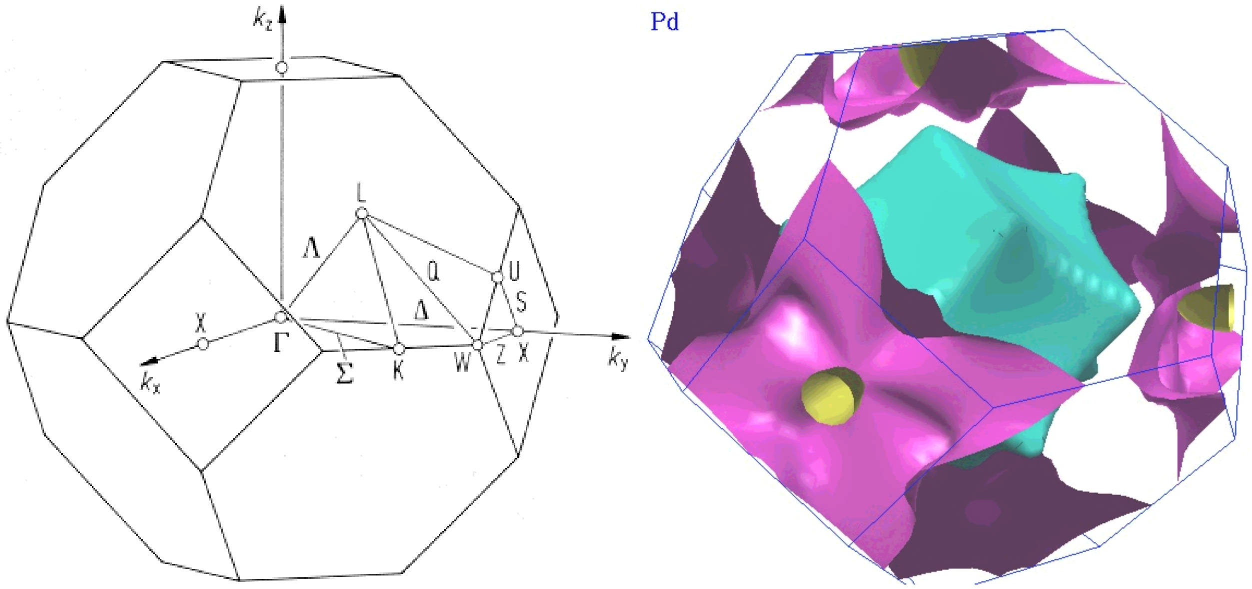

The whole situation is somewhat confused because of the presence of a so-called **hybridisation gap** between one of the d-bands and the broad s-band. In Fig. V.2 we show schematically the effect of hybridisation.

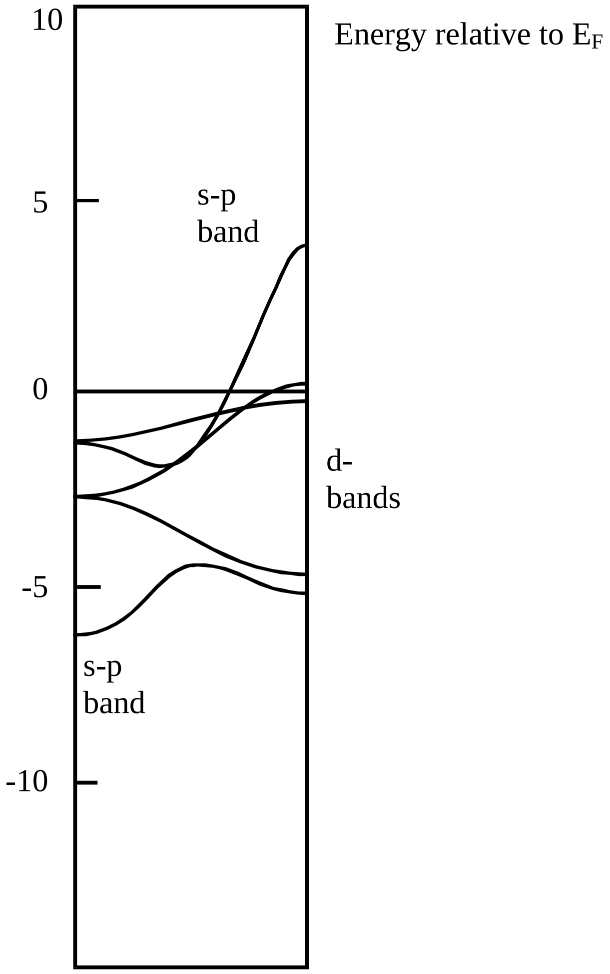

Fig. V.2: Effect of hybridisation between one of the d-states with the s-p-band. Left panel: with hybridisation; Right panel: without hybridisation (the hybridised bands are given as dashed lines).

V.3 TIGHT-BINDING APPROXIMATION

We shall now show that it is possible to understand what seems to be very complex, the E(**k**) along the ΓX direction in FCC metals, by means of a simple calculation based on the tight-binding approximation (TBA).

In the TBA one assumes that the crystal wave function $\Psi_{\mathbf{k}}$ which satisfies the Schrödinger equation for one electron in the whole crystal

$$H\Psi_{\mathbf{k}}(\mathbf{r}) = E_{\mathbf{k}}\Psi_{\mathbf{k}}(\mathbf{r}) \qquad \text{(V.1}$$

may be represented as a combination of atomic wave functions $\varphi_j(\mathbf{r}-\mathbf{R})$ located at the position $\mathbf{R}$ of the atoms and satisfying the atomic Schrödinger equation

$$H_{atomic}\varphi_j = E_j\varphi_j \qquad \text{(V.2}$$

We seek a solution of Eq.V.1 in the form

$$\Psi_{\mathbf{k}}(\mathbf{r}) = \underset{\text{sum over all atomic sites}}{\sum_{\mathbf{R}}} e^{i\mathbf{k}\cdot\mathbf{R}} \sum_j c_j\varphi_j(\mathbf{r}-\mathbf{R}) \qquad \text{(V.3}$$

This combination is chosen in such a way as to satisfy Bloch's theorem

$$\Psi_{\mathbf{k}}(\mathbf{r}+\mathbf{R}_0) = e^{i\mathbf{k}\cdot\mathbf{R}_0}\Psi_{\mathbf{k}}(\mathbf{r}) \qquad \text{for all } \mathbf{R_0} \qquad \text{(V.4}$$

The proof is immediate. From Eq.V.3 follows that

$$\begin{aligned}
\Psi_{\mathbf{k}}(\mathbf{r}+\mathbf{R}_0) &= \sum_{\mathbf{R}} e^{i\mathbf{k}\mathbf{R}} \sum_j c_j\varphi_j(\mathbf{r}+\mathbf{R}_0-\mathbf{R}) \\
&= e^{i\mathbf{k}\cdot\mathbf{R}_0} \sum_{\mathbf{R}} e^{i\mathbf{k}\cdot(\mathbf{R}-\mathbf{R}_0)} \sum_j c_j\varphi_j(\mathbf{r}+\mathbf{R}_0-\mathbf{R}) \qquad \text{(V.5} \\
&= e^{i\mathbf{k}\cdot\mathbf{R}_0} \underbrace{\sum_{\Box} e^{i\mathbf{k}\cdot\rho} \sum_j c_j\varphi_j(\mathbf{r}-\rho)}_{\Psi_{\mathbf{k}}(\mathbf{r})} \qquad \textit{Q.E.D.}
\end{aligned}$$

We shall now represent the Schrödinger equation, Eq.V.1, in a matrix form. For this, we multiply Eq.V.1 by an atomic function $\varphi_m(r)$ (φ_m is real)

$$\varphi_m(\mathbf{r})H\Psi_{\mathbf{k}}(\mathbf{r}) = E_{\mathbf{k}}\varphi_m(\mathbf{r})\Psi_{\mathbf{k}}(\mathbf{r}) \qquad \text{(V.6}$$

and integrate over the volume of the sample to obtain

$$\langle\varphi_m(\mathbf{r})|H|\Psi_{\mathbf{k}}(\mathbf{r})\rangle = E_{\mathbf{k}}\langle\varphi_m(\mathbf{r})|\Psi_{\mathbf{k}}(\mathbf{r})\rangle \qquad \text{(V.7}$$

In what follows we shall make use of the orthogonality of the $\varphi_j(r)$ located at the same atomic site, i.e.

$$\left\langle \varphi_m(\mathbf{r}) \middle| \varphi_j(\mathbf{r}) \right\rangle = \delta_{mj} \qquad \text{(V.8}$$

and assume that because of the small overlap between φ's on different atomic sites, we have the following quasi-orthogonality condition

$$\left\langle \varphi_j(\mathbf{r}) \middle| \varphi_m(\mathbf{r}+\mathbf{R}) \right\rangle \cong \delta_{R=0}\delta_{jm} \qquad \text{(V.9}$$

This is exactly what we did in the treatment of the H_2^+ and the H_2 molecules in Chapter II. Then Eq.V.6 can be written in the following way

$$\begin{aligned}
\left\langle \varphi_m(\mathbf{r}) \middle| H \middle| \Psi_k(\mathbf{r}) \right\rangle &= \sum_R e^{i\mathbf{k}\cdot\mathbf{R}} \sum_{j=1}^{L} c_j \left\langle \varphi_m(\mathbf{r}) \middle| H \middle| \varphi_j(\mathbf{r}-\mathbf{R}) \right\rangle \\
&= \sum_{j=1}^{L} c_j \left[\sum_R e^{i\mathbf{k}\cdot\mathbf{R}} \left\langle \varphi_m(\mathbf{r}) \middle| H \middle| \varphi_j(\mathbf{r}-\mathbf{R}) \right\rangle \right] \\
&= E_k \sum_j c_j \left[\sum_R e^{i\mathbf{k}\cdot\mathbf{R}} \left\langle \varphi_m(\mathbf{r}) \middle| \varphi_j(\mathbf{r}-\mathbf{R}) \right\rangle \right] \\
&\cong E_k c_m
\end{aligned} \qquad \text{(V.10}$$

In matrix notation we obtain

$$\begin{bmatrix}
\sum\limits_R e^{i\mathbf{k}\cdot\mathbf{R}} \left\langle \varphi_1(\mathbf{r}) \middle| H \middle| \varphi_1(\mathbf{r}-\mathbf{R}) \right\rangle & \cdots & \sum\limits_R e^{i\mathbf{k}\cdot\mathbf{R}} \left\langle \varphi_L(\mathbf{r}) \middle| H \middle| \varphi_1(\mathbf{r}-\mathbf{R}) \right\rangle \\
\vdots & \ddots & \vdots \\
\sum\limits_R e^{i\mathbf{k}\cdot\mathbf{R}} \left\langle \varphi_1(\mathbf{r}) \middle| H \middle| \varphi_L(\mathbf{r}-\mathbf{R}) \right\rangle & \cdots & \sum\limits_R e^{i\mathbf{k}\cdot\mathbf{R}} \left\langle \varphi_L(\mathbf{r}) \middle| H \middle| \varphi_L(\mathbf{r}-\mathbf{R}) \right\rangle
\end{bmatrix}
\begin{bmatrix} c_1 \\ \vdots \\ c_L \end{bmatrix} \cong E_k \begin{bmatrix} c_1 \\ \vdots \\ c_L \end{bmatrix} \qquad \text{(V.11}$$

Close to an atom (which for simplicity of notation is assumed to be at $R_0=0$) the crystal potential resembles strongly the atomic potential (see Fig.V.3) and we write

$$H = H_{atomic} + h \qquad \text{(V.12}$$

where *h* is small in the vicinity of $R_0=0$. Then

$$\left\langle \varphi_m(\mathbf{r}) \middle| H \middle| \varphi_j(\mathbf{r}-\mathbf{R}) \right\rangle = \left\langle \varphi_m(\mathbf{r}) \middle| H_{atomic} \middle| \varphi_j(\mathbf{r}-\mathbf{R}) \right\rangle + \left\langle \varphi_m(\mathbf{r}) \middle| h \middle| \varphi_j(\mathbf{r}-\mathbf{R}) \right\rangle \qquad \text{(V.13}$$

From Eq.V.2 follows that

$$\begin{aligned}
\left\langle \varphi_m(\mathbf{r}) \middle| H_{atomic} \middle| \varphi_j(\mathbf{r}-\mathbf{R}) \right\rangle &= E_j \left\langle \varphi_m(\mathbf{r}) \middle| \varphi_j(\mathbf{r}-\mathbf{R}) \right\rangle \\
&= E_j \delta_{mj} \delta_{R=0}
\end{aligned} \qquad \text{(V.14}$$

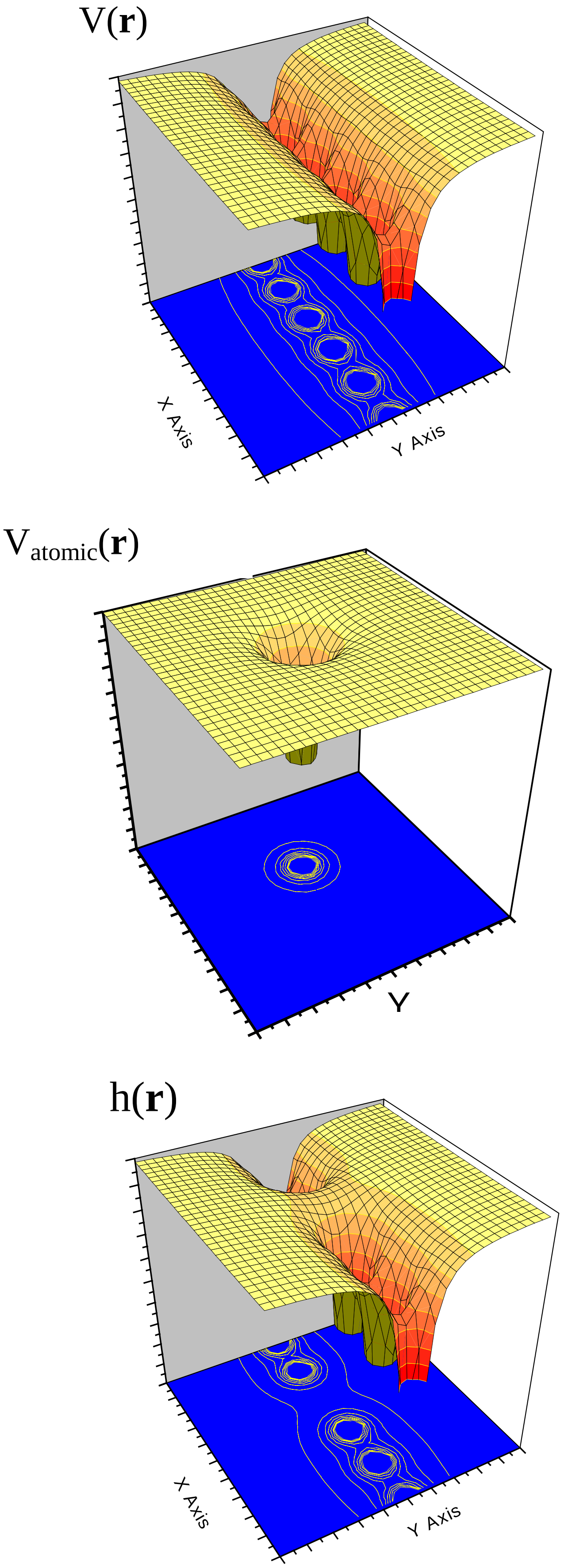

Fig.V.3: In the tight-binding approximation the periodic potential due to the atoms in a chain of atoms is split into an atomic potential V_{atomic} at a chosen place and a potential h(r) that is weak near the chosen location.

Denoting the overlap integral $\langle \varphi_m(\mathbf{r}) | h | \varphi_j(\mathbf{r}-\mathbf{R}) \rangle$ by $B_{mj}(\mathbf{R})$ we have finally (from Eq.V.9),

$$\begin{aligned}
&\sum_j c_j \left[\sum_{\mathbf{R}} e^{i\mathbf{k}\cdot\mathbf{R}} \left(E_j \delta_{mj} \delta_{R=0} + B_{mj}(\mathbf{R}) \right) \right] = \\
&\sum_j c_j \left[E_j \delta_{mj} + \sum_{\mathbf{R}} e^{i\mathbf{k}\cdot\mathbf{R}} B_{mj}(\mathbf{R}) \right] = E_k c_m
\end{aligned} \qquad \text{(V.15}$$

In matrix notation

$$\begin{bmatrix} E_m + \sum_{\mathbf{R}} e^{i\mathbf{k}\cdot\mathbf{R}} B_{11}(\mathbf{R}) & \cdots & \sum_{\mathbf{R}} e^{i\mathbf{k}\cdot\mathbf{R}} B_{1L}(\mathbf{R}) \\ \vdots & \ddots & \vdots \\ \sum_{\mathbf{R}} e^{i\mathbf{k}\cdot\mathbf{R}} B_{L1}(\mathbf{R}) & \cdots & E_j + \sum_{\mathbf{R}} e^{i\mathbf{k}\cdot\mathbf{R}} B_{LL}(\mathbf{R}) \end{bmatrix} \begin{bmatrix} c_1 \\ \vdots \\ c_L \end{bmatrix} \cong E_k \begin{bmatrix} c_1 \\ \vdots \\ c_L \end{bmatrix} \qquad \text{(V.16}$$

This system of equations has a non-trivial solution if the determinant of the matrix vanishes

$$\begin{vmatrix} E_1 - E_k + \sum_{\mathbf{R}} e^{i\mathbf{k}\cdot\mathbf{R}} B_{11}(\mathbf{R}) & \cdots & \sum_{\mathbf{R}} e^{i\mathbf{k}\cdot\mathbf{R}} B_{1L}(\mathbf{R}) \\ \vdots & \ddots & \vdots \\ \sum_{\mathbf{R}} e^{i\mathbf{k}\cdot\mathbf{R}} B_{L1}(\mathbf{R}) & \cdots & E_j - E_k + \sum_{\mathbf{R}} e^{i\mathbf{k}\cdot\mathbf{R}} B_{LL}(\mathbf{R}) \end{vmatrix} = 0 \qquad \text{(V.17}$$

To make contact with the band structure shown in Fig. V.1 we shall specialise this equation to the case of one s-band and five d-bands ($(2\ell+1)=5$ for d-states ($\ell=2$)).

We evaluate now the matrix elements for the case where **k** is parallel to the [001] direction. The reason for choosing this particular situation is that the matrix in Eq.V.16 takes a simple form (almost diagonal) for this direction. This is related to the fact that the z-axis is normally chosen as the quantisation direction when solving the atomic problem $H_{\text{atomic}}\varphi_j = E_j\varphi_j$.

Let us first focus our attention on the 5×5 matrix describing d-states, which takes the following diagonal form when k||z-axis

$$\begin{bmatrix} E_d - E_k + \sum_{\mathbf{R}} e^{i\mathbf{k}\cdot\mathbf{R}} B_{11} & & \varnothing \\ & \ddots & \\ \varnothing & & E_d - E_k + \sum_{\mathbf{R}} e^{i\mathbf{k}\cdot\mathbf{R}} B_{55} \end{bmatrix} \qquad \text{(V.18}$$

We shall not give a general proof that the matrix is diagonal but just show that some matrix elements vanish. For example, for the matrix element (yz, $3z^2$-r^2) in the case of a FCC crystal, we have the situation shown in Fig. V.4. The matrix being diagonal we can immediately write the equations for the 5 d-bands as

$$\begin{aligned} E_k &= E_d + \sum_{\mathbf{R}} e^{i\mathbf{k}\cdot\mathbf{R}} B_{jj}(\mathbf{R}) \\ &= E_d + 2\sum\nolimits^{*} \cos(\mathbf{k}\cdot\mathbf{R}) B_{jj}(\mathbf{R}) \end{aligned} \tag{V.19}$$

where Σ^* is a sum over the z>0 half space (we have made use of the symmetry of $B_{jj}(\mathbf{R}) = B_{jj}(-\mathbf{R})$).

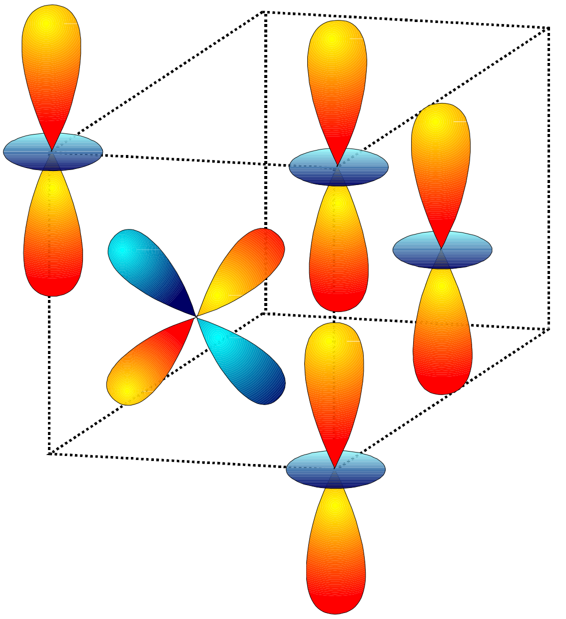

Fig. V.4: Schematic drawing showing that the matrix element between a $3z^2$-r^2 state and an yz state vanishes for a metal with FCC crystal structure.

The integral B_{jj} are usually complicated to evaluate. For the purpose of our qualitative discussion we consider now the simplest case which is that of BCC metals (e.g. Niobium) when only nearest-neighbour overlap integrals are considered. We have then the situations shown in Fig. V.5 and Fig. V.6. From these figures it is easy to see that

$$sign\left(B_{yz,yz}\right) = -sign\left(B_{x^2-y^2,x^2-y^2}\right) \tag{V.20}$$

It can also be shown that for nearest neighbours

$$B_{yx,yx} = B_{yz,yz} = B_{xz,xz} \tag{V.21}$$

and that

$$B_{x^2-y^2,x^2-y^2} = B_{3z^2-r^2,3z^2-r^2} \tag{V.22}$$

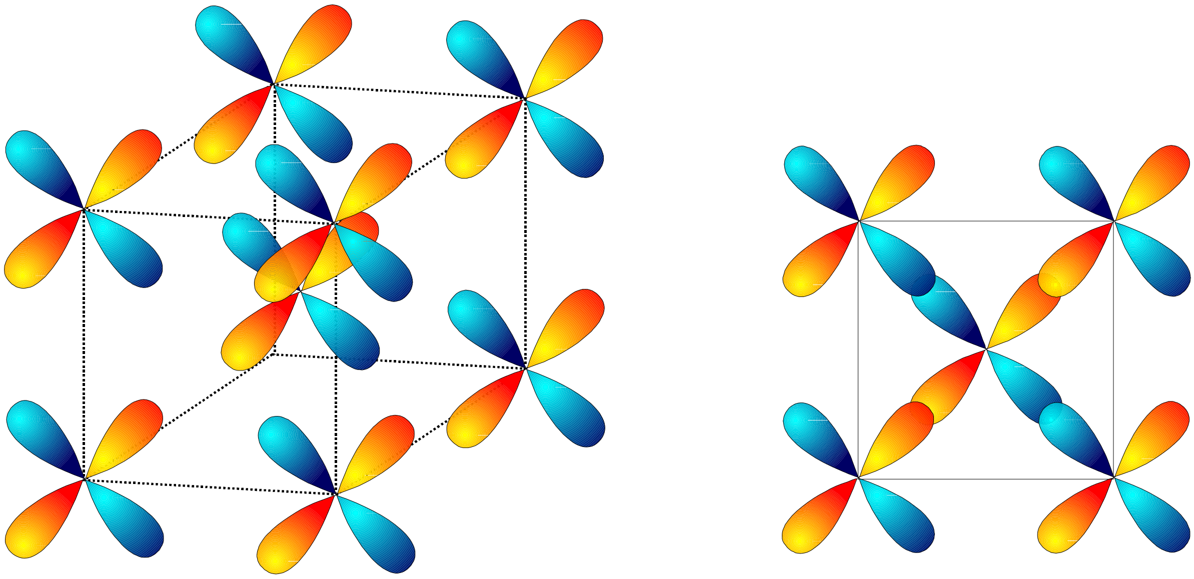

Fig. V.5: Schematic drawing required to show that the sign of $B_{yz,yz}$ is opposite to that of $B_{x^2-y^2,\, x^2-y^2}$ in a BCC structure. The right panel is a projection of the left panel onto the (y,z)-plane.

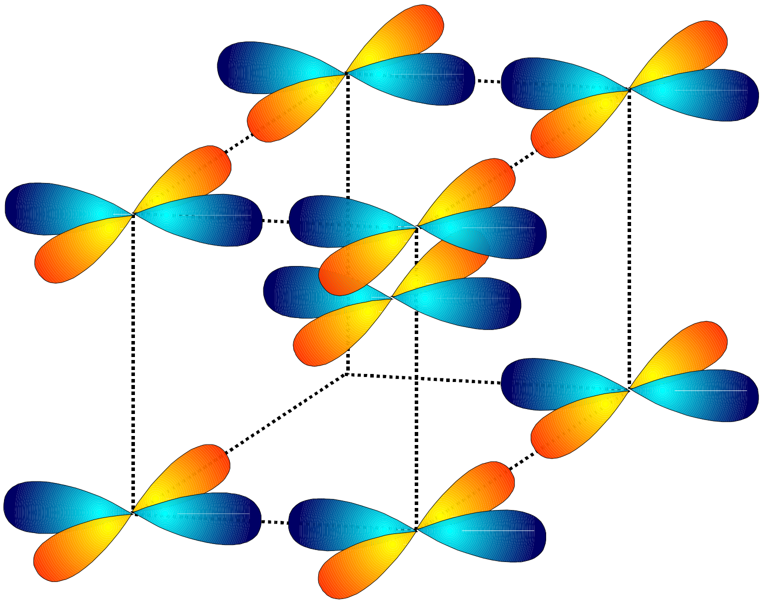

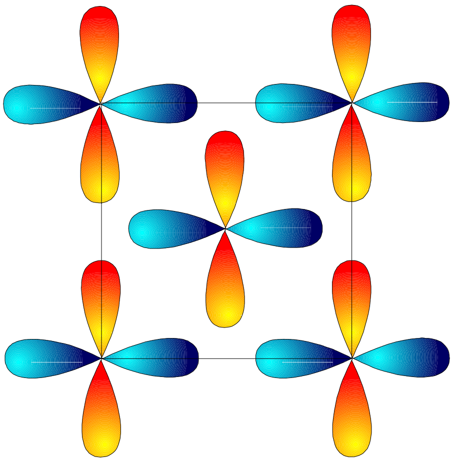

Fig. V.6: Schematic drawing required to show that the sign of $B_{yz,yz}$ is opposite to that of $B_{x^2-y^2,\, x^2-y^2}$ in a BCC structure. The right panel is a projection of the left panel onto the (x,y)-plane.

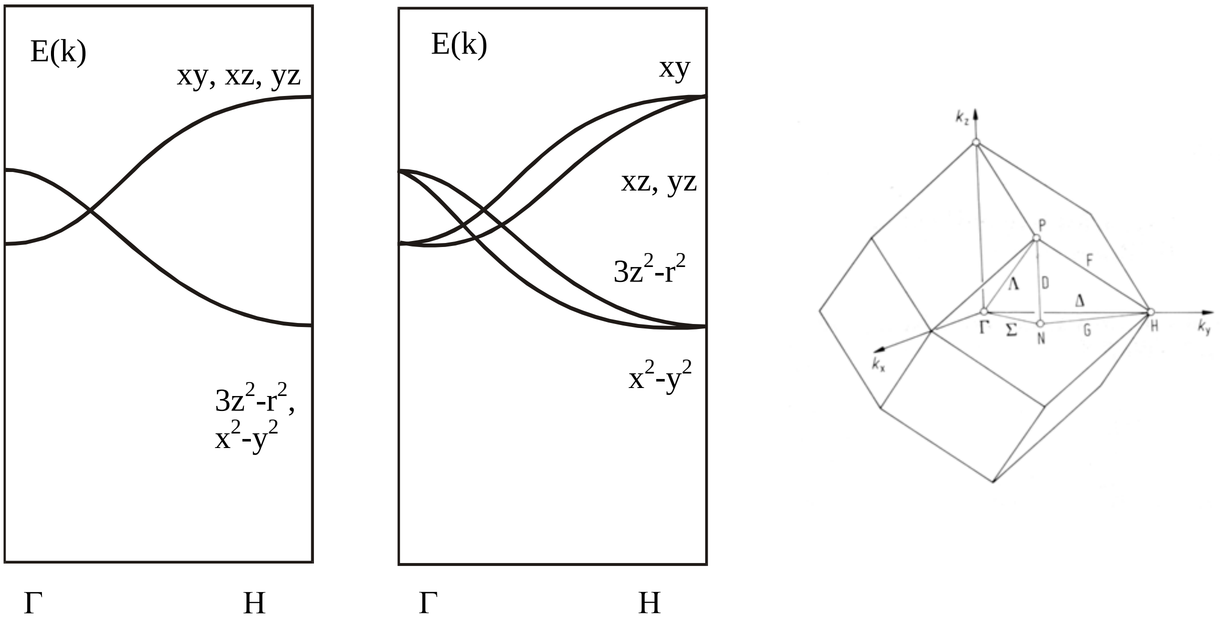

Fig. V.7: d-band structure of a metal with a BCC lattice. In the left panel only first nearest neighbour overlaps are considered. In the right panel second nearest neighbour overlap integrals are included. The Brillouin zone of the BCC lattice is shown on the right.

In the ΓH direction ([001]) of the Brillouin zone shown in Fig. V.7 we have thus two sets of bands i) a doubly degenerated set and ii) a triply degenerated set.

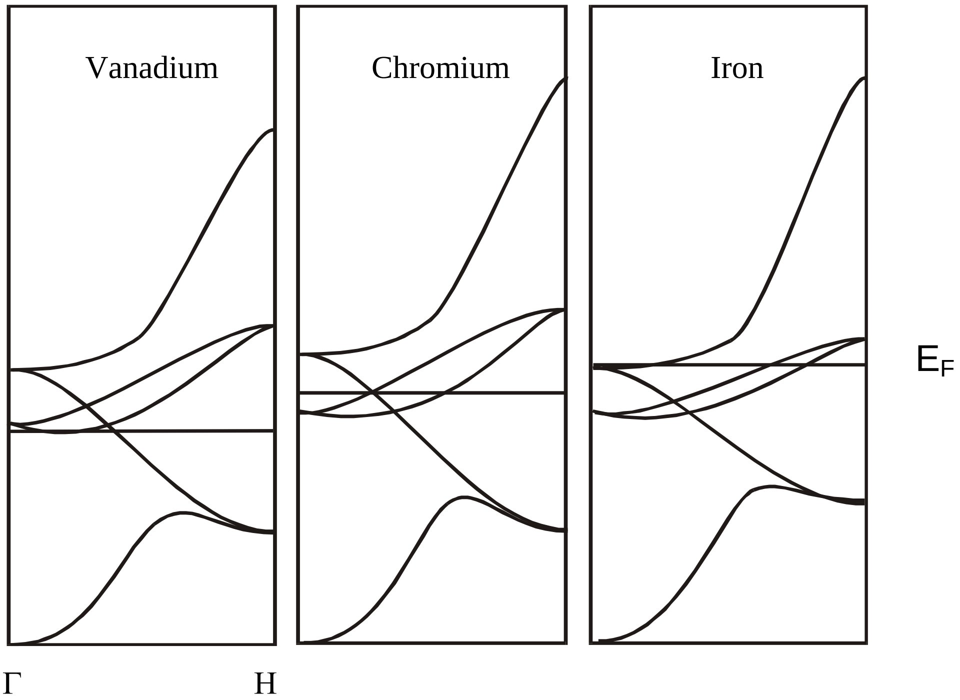

Fig. V.8: Band structure along ΓH (see Fig. V.7) of three representative metals with a BCC lattice. Except for the strong hybridisation of the $3z^2$-r^2 d-state with the s-p-states these calculations are similar to those indicated schematically in Fig. V.7. The Fermi energy is indicated by a horizontal line.

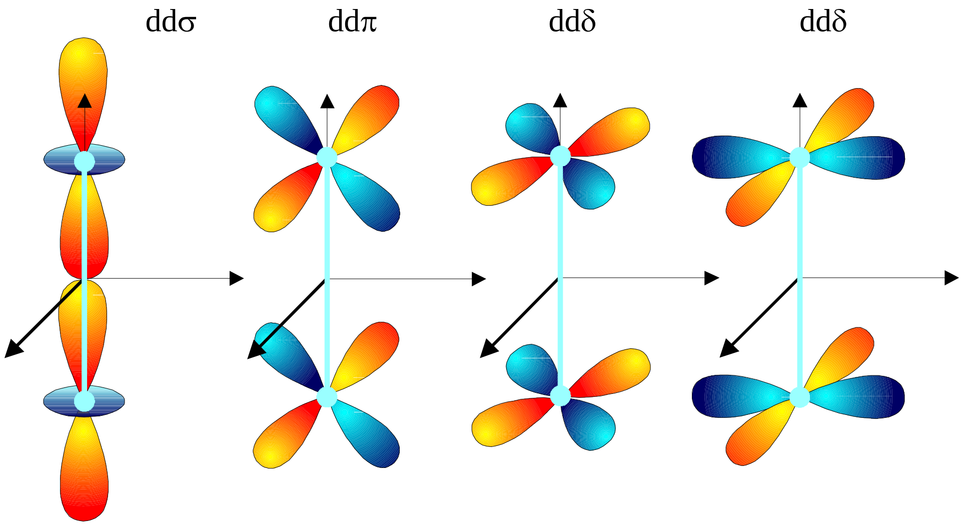

Table V.1: Overlap integrals after Slater and Koster[3]. (l, m, n) are the direction cosines of the lattice vector **R.** The fundamental overlap integrals ddσ, ddπ and ddδ are shown at the top of this page. The distance between the atomic wave functions is R.

$B_{xy,\, xy}$	$3\, l^2m^2\, \mathrm{dd}\sigma +(l^2+m^2-4\, l^2\, m^2)\, \mathrm{dd}\pi + (n^2+l^2\, m^2)\, \mathrm{dd}\delta$
$B_{xy,\, yz}$	$3\, l^2\, m^2 n\, \mathrm{dd}\sigma + ln(1-4\, m^2)\, \mathrm{dd}\pi + ln(m^2-1)\, \mathrm{dd}\delta$
$B_{xy,\, xz}$	$3\, l^2 mn\, \mathrm{dd}\sigma +(1-4\, l^2)\, \mathrm{dd}\pi + mn(l^2-1)\, \mathrm{dd}\delta$
$B_{xy,\, x^2-y^2}$	$(3/2)lm\, (l^2-m^2)\, \mathrm{dd}\sigma +2lm(m^2-l^2)\, \mathrm{dd}\pi + (1/2)lm(l^2-m^2)\, \mathrm{dd}\delta$
$B_{yz,\, x^2-y^2}$	$(3/2)mn\, (l^2-m^2)\, \mathrm{dd}\sigma -mn[1+2(l^2-m^2)]\mathrm{dd}\pi + mn[1+(1/2)(l^2-m^2)]\, \mathrm{dd}\delta$
$B_{xz,\, x^2-y^2}$	$(3/2)nl\, (l^2-m^2)\, \mathrm{dd}\sigma -nl[1-2(l^2-m^2)]\mathrm{dd}\pi - nl[1-(1/2)(l^2-m^2)]\, \mathrm{dd}\delta$
$B_{xy,\, 3z^2-r^2}$	$\sqrt{3}\, lm[n^2-(1/2)(l^2+m^2)]\, \mathrm{dd}\sigma -2\sqrt{3}\, lmn^2\, \mathrm{dd}\pi + (1/2)\sqrt{3}\, (1+n^2)\, \mathrm{dd}\delta$
$B_{yz,\, 3z^2-r^2}$	$\sqrt{3}mn[n^2-(1/2)(l^2+m^2)]\, \mathrm{dd}\sigma +\sqrt{3}\, mn(l^2+m^2-n^2)\, \mathrm{dd}\pi$ $- (1/2)\sqrt{3}mn\, (l^2+m^2)\, \mathrm{dd}\delta$
$B_{xz,\, 3z^2-r^2}$	$\sqrt{3}ln[n^2-(1/2)(l^2+m^2)]\, \mathrm{dd}\sigma +\sqrt{3}\, ln(l^2+m^2-n^2)\, \mathrm{dd}\pi$ $- (1/2)\sqrt{3}ln\, (l^2+m^2)\, \mathrm{dd}\delta$
$B_{x^2-y^2,\, x^2-y^2}$	$(3/4)(l^2-m^2)^2\, \mathrm{dd}\sigma +[l^2+m^2-(l^2-m^2)^2]\mathrm{dd}\pi +[n^2+(1/4)(l^2-m^2)^2]\, \mathrm{dd}\delta$
$B_{x^2-y^2,\, 3z^2-r^2}$	$(\sqrt{3}/2)(l^2-m^2)\, [n^2-(1/2)(l^2+m^2)]\, \mathrm{dd}\sigma +\sqrt{3}n^2\, (m^2-l^2)\,]\mathrm{dd}\pi$ $+[(1+n^2)\, (l^2-m^2)]\, \mathrm{dd}\delta$
$B_{3z^2-r^2,\, 3z^2-r^2}$	$[n^2-(1/2)(l^2+m^2)]^2\, \mathrm{dd}\sigma +3n^2\, (l^2+m^2)\, \mathrm{dd}\pi + (3/4)(l^2+m^2)^2\, \mathrm{dd}\delta$

For the FCC metals the situation is more difficult and one uses the Slater-Koster tables to express the overlap integrals $B_{jm}(\mathbf{R})$ in terms of simpler overlap integrals that depend only on the magnitude R of **R**. For the case of d-atomic functions, these simpler overlap integrals are written ddσ, ddπ and ddδ and

$$B_{jm}(\mathbf{R}) = B_{jm}\left(dd\sigma(R), dd\pi(R), dd\delta(R), \alpha, \beta, \gamma\right) \qquad \text{(V.23}$$

where α, β, γ are the angles with direction cosine *l, m, n* which correspond to **R**. For explicit relations see Table V.1. With these tables one can construct the 5×5 matrix completely and for FCC structures one finds, including only first nearest-neighbours, that the band structure in the ΓX direction is as indicated in Fig. V.9.

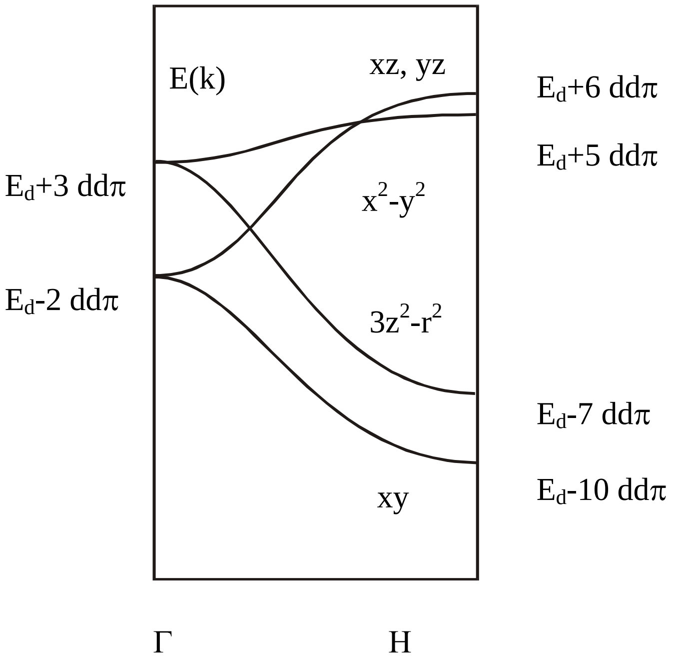

Fig. V.9: d-band structure of a metal with a FCC lattice when only nearest neighbour overlaps are taken into account. From a comparison with the band structure of Pd in Fig.V.1 we conclude that the main features (except for the hybridisation between the $3z^2$-r^2 d-state and the s-p- states) are well reproduced. For the drawing we have used the fact that approximately ddσ = -2 ddπ >>ddδ

V.4 S-D HYBRIDISATION

We see that for d-bands we obtain quite easily the correct shape by means of a very simple calculation. Let us now come back to our original problem, which includes 5-d-bands **and** a s-band. Here we have to look at the matrix elements between s and d-wave functions. All are zero except one. This is illustrated in Fig. V.10.

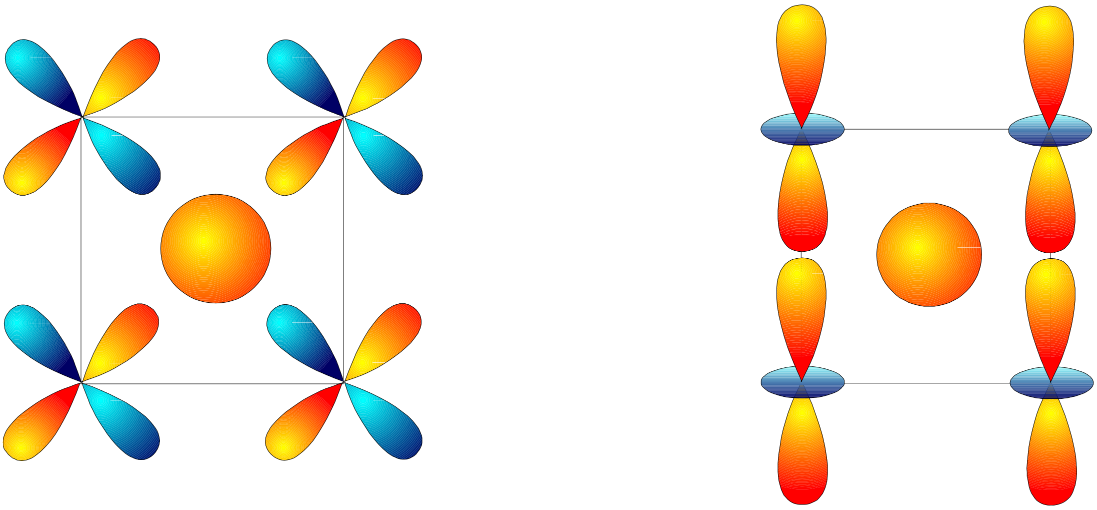

Fig. V.10: (Left panel) Example of a situation where the s-d-overlap vanishes. The d-state is here of the yz-form. (Right panel). Example of a situation where the s-d-overlap is large. The d-state is here of the $3z^2$-r^2 form. Note that for an observer at the center of the square the 4 d-wave functions form an environment with predominantly s-symmetry !

The matrix Eq.V.17 has thus the following form

$$\left[\begin{array}{c:cccccc}
E_s - E_k + \sum\limits_{\mathbf{R}} e^{i\mathbf{k}\cdot\mathbf{R}} B_{ss} & 0 & 0 & \sum\limits_{\mathbf{R}} e^{i\mathbf{k}\cdot\mathbf{R}} B_{s,3z^2-r^2} & 0 & 0 \\
\hdashline
 & \ddots & & \vdots & & \\
 & & \ddots & \vdots & \varnothing & \\
 & & & E_d - E_k + \sum\limits_{\mathbf{R}} e^{i\mathbf{k}\cdot\mathbf{R}} B_{3z^2-r^2,3z^2-r^2}(\mathbf{R}) & & \\
 & & \varnothing & & \ddots & \\
 & & & & & \ddots
\end{array}\right] \quad \text{(V.24}$$

Let us now investigate the effect of the hybridisation term containing $B_{s,3z2\text{-}r2}$. This term couples an s-state with the $3z^2$-r^2 d-state. To simplify the algebra we consider the case near $E_s=E_d=E_0$. The s- and d-bands cross each other and, locally, E(**k**) varies linearly with **k**. We write

$$\begin{aligned} E_s(\mathbf{k}) &\cong E_0 + \alpha(k-k_0) \quad \text{with } \alpha \geq 0 \\ E_d(\mathbf{k}) &\cong E_0 + \beta(k-k_0) \quad \text{with } \beta \leq 0 \end{aligned} \quad \text{(V.25}$$

as we are just interested in the region close to the crossing point. We have then to solve the following 2×2 secular equation

$$\begin{vmatrix} E_0 - E_k + \alpha(k-k_0) & W \\ W & E_0 - E_k + \beta(k-k_0) \end{vmatrix} = 0 \quad \text{(V.26}$$

where $W=\sum_{\mathbf{R}} e^{i\mathbf{k}\cdot\mathbf{R}} B_{s,3z^2-r^2}$ is assumed to be constant for k≅k$_0$. The solution of Eq.V.26 is simply

$$E_k = E_0 + \frac{(\alpha+\beta)(k-k_0) \pm \sqrt{(\alpha-\beta)^2 (k-k_0)^2 + 4W^2}}{2} \qquad \text{(V.27}$$

For k=k$_0$ we have

$$E_{k_0} = E_0 \pm |W| \qquad \text{(V.28}$$

which means that a gap has opened at k=k$_0$, i.e. the two bands do not cross any longer.

For $(k-k_0)^2(\alpha-\beta)^2 » 4W^2$, E_k joins smoothly the original $E_s(\mathbf{k})$ and $E_d(\mathbf{k})$ curves. Note, however, that in most transition metals the hybridisation gap is of the same order as the width of the d-band. This is clearly visible in Fig.V.1 for the case of palladium.

To have a better feeling for what happens near the hybridisation gap let us look at the wave functions for k=k$_0$. We have, since W>0 (see right panel in Fig. V.10)

$$c_s = \mp c_d \qquad \text{(V.29}$$

For the lower band we have to take the + sign (see Eq.V.28) and thus the wave function is the sum of an s and a $3z^2$-r^2 - functions.

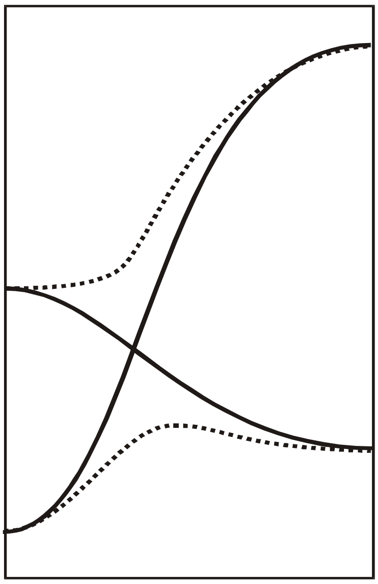

Fig. V.11: Hybridisation between the $3z^2$-r^2 d-state and an s-state. Full lines: unhybridised bands; Dashed lines: hybridised bands.

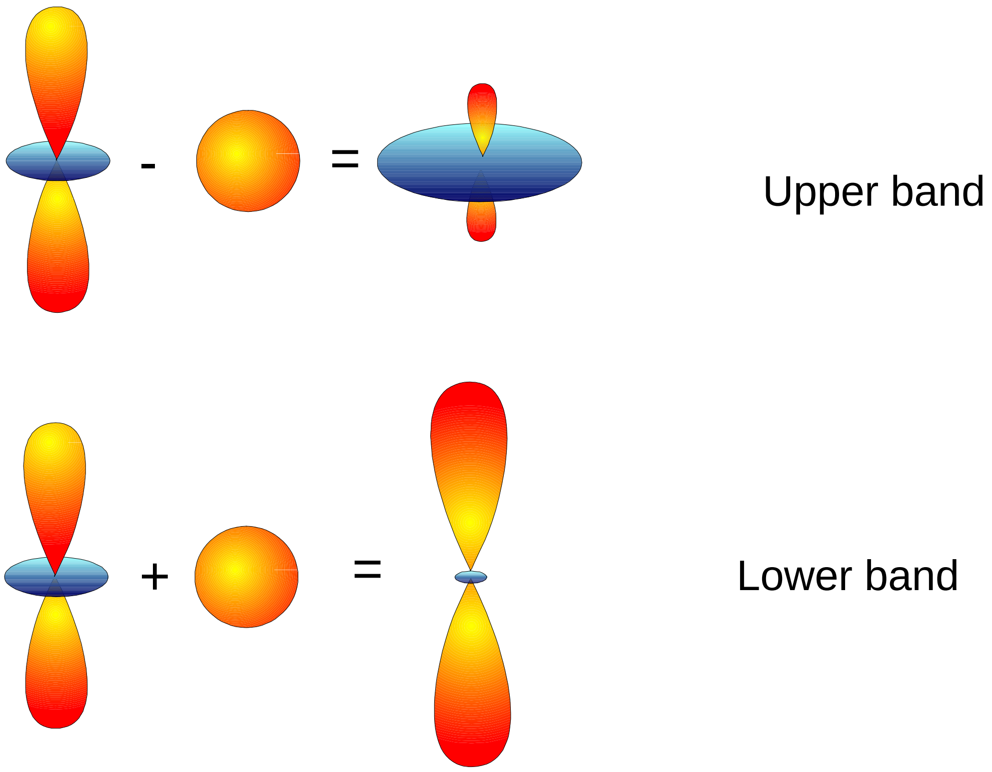

We have now all the ingredients necessary for a qualitative discussion of the effect of hydrogen (or any other interstitial impurity) on the band structure of a transition metal.

V.5 EFFECT OF H ON THE BAND STRUCTURE OF A METAL

The objective of this section is to develop a qualitative understanding of the main influence of hydrogen on the electronic states of the host metal. As a concrete example we consider the band structure calculated by Moruzzi[1] for stoichiometric PdH shown in Fig. V.12. From a comparison of this figure with the band structure of pure Palladium shown in Fig,V.1 one notices three important changes:

- the lowest band is lowered by 3 eV almost everywhere in the whole Brillouin zone when hydrogen is added to Pd.
- the Fermi energy has been pushed above the d-band complex
- the s-p band above the d-band has been lowered somewhat. The shift is, however, significantly smaller than that of the lowest band.
- the width of the d-band is reduced with respect to that of pure Pd.

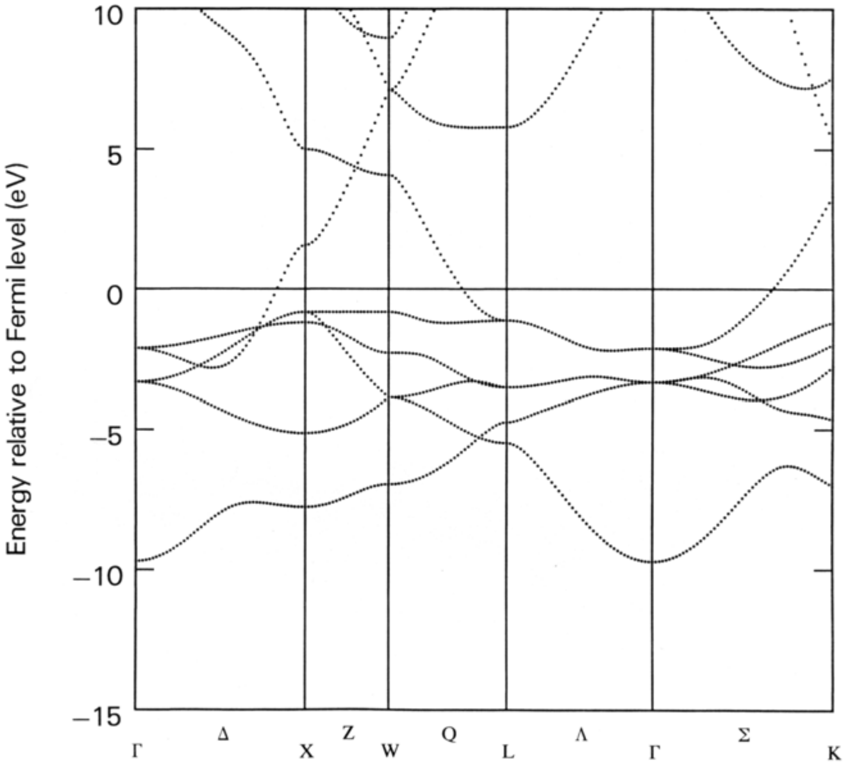

Fig. V.12: Band structure of PdH. The meaning of the symbols is explained in Fig. V.1.

As in the main part of this chapter we shall base our argument on a schematic picture of the wave function and use first order perturbation theory to evaluate the shifts in energy $\langle\Psi_k|V_H|\Psi_k\rangle$ at several representative points in the Brillouin zone. V_H is the perturbation in the crystal potential induced by the presence of a proton in the host metal lattice.

V.5.1 S-BAND AT POINT Γ AND AT POINT X

At the centre of the Brillouin zone, k=0, and from Eq.V.3 and the fact that hybridisation is relatively weak for **k**≅0 we see that the s-wave function is given by

$$\Psi_{\mathbf{k}=0}(\mathbf{r}) = \sum_{\mathbf{R}} e^{i\mathbf{k}\cdot\mathbf{R}}\varphi_s(\mathbf{r}-\mathbf{R}) = \sum_{\mathbf{R}}\varphi_s(\mathbf{r}-\mathbf{R}) \qquad \text{(V.30}$$

It is just a superposition of s-atomic wave functions. From Fig. V.13 one sees immediately that the energy shift

$$\Delta E_s(k=0) = \left\langle \Psi_{\mathbf{k}=0,s} \middle| V_H \middle| \Psi_{\mathbf{k}=0,s} \right\rangle \qquad \text{(V.31}$$

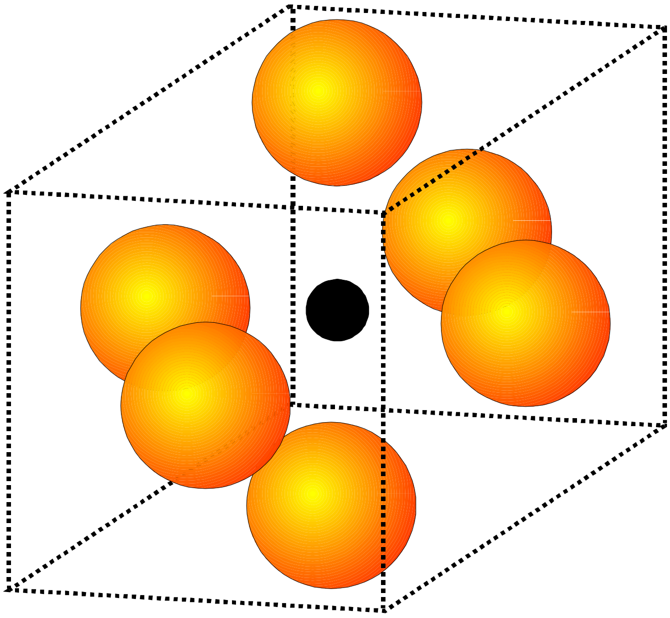

Fig. V.13: The **k**=0, s-wave function in a FCC metal such as Pd. At **k**=0 the phase factors in Eq.V.3 are all equal to 1. The proton is indicated as a black dot at one of the octahedral interstitial sites. There is a substantial s-s overlap at the site of the proton, and consequently $\Delta E_{\mathbf{k}=0}$ is large for this s-state

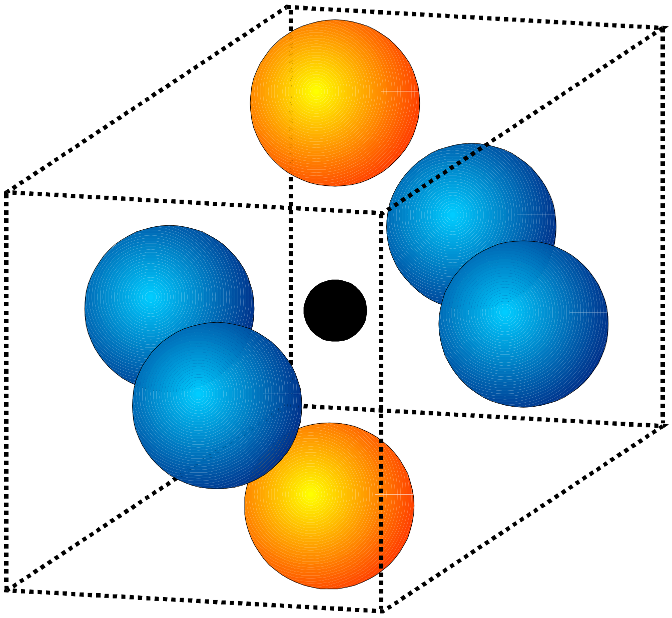

Fig. V.14: As in Fig.V.16 but now for **k**=(0, 0, 2π/a), which corresponds to point X in the Brillouin zone. The phase factors in Eq.V.3 alternate between +1 and -1. It follows immediately that $\Delta E_{\mathbf{k}=(0,\ 0,\ 2\pi/a)}$ is nine times smaller than $\Delta E_{\mathbf{k}=0}$.

is quite important because of the substantial overlap of the $\varphi_s(\mathbf{r}-\mathbf{R})$ wave functions at the octahedral interstitial sites in the case of a FCC metal. At the top of the s-band we have the situation shown in Fig. V.14. Since now the phase factors in Eq.V.3 alternate in sign the overlap of the proton potential with 2 positive and 4 negative atomic wave functions is three times smaller than at the bottom of the band. The energy shift induced by the proton is thus 9 times smaller in qualitative agreement with the band structure calculations (compare Fig. V.1 and Fig. V.12).

These conclusions remain valid even at $\mathbf{k}\cong\mathbf{k}_0$, where the overlap of the Ψ^-_{k0} wave function is much more important than that of the $\Psi^+_{\mathbf{k}0}$ wave function. As a result of this, the lowest band in Pd-H is almost rigidly lowered by ~ 3 eV.

V.5.2 D-BANDS AT POINT Γ AND AT POINT X

Let us now discuss the influence of H on pure d-states. According to the calculation of Moruzzi[1] the d-bands are virtually unaffected by the interstitial hydrogen. The reason for this is easily seen in Fig. V.15 and Fig. V.16.

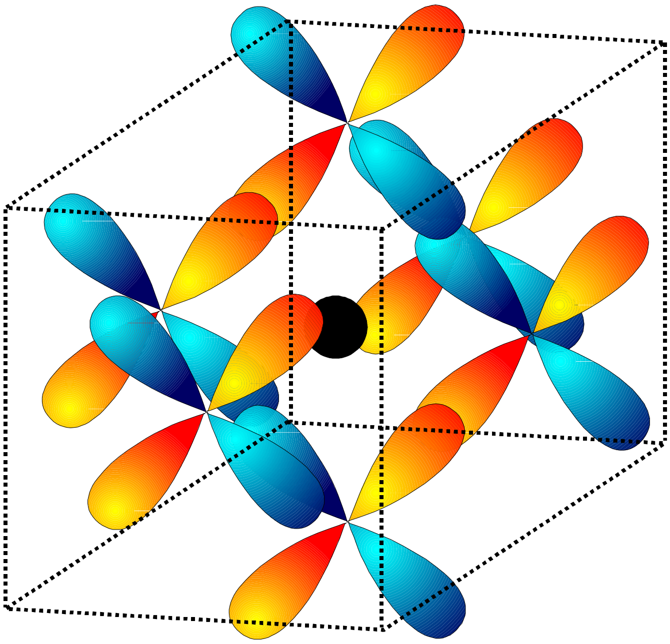

Fig. V.15: The **k**=0, d-wave function with yz-symmetry has zero amplitude exactly at the octahedral site. The energy shift $\Delta E_{\mathbf{k}=0}$ is very small for this d-state.

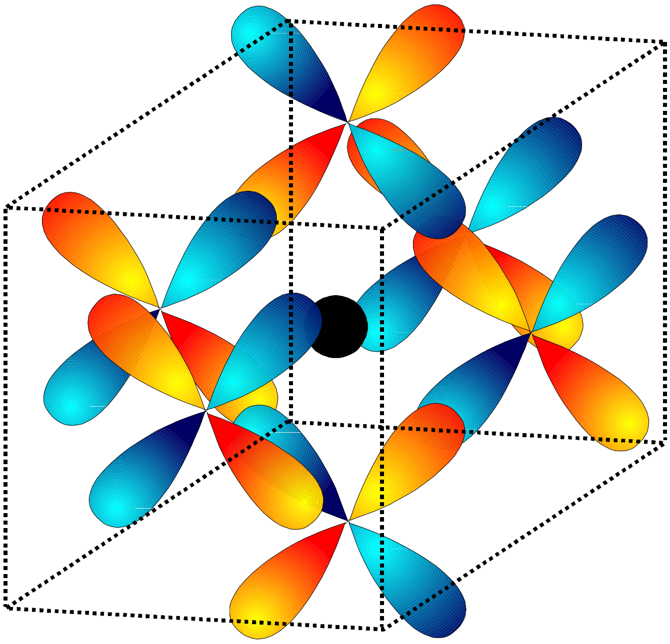

Fig. V.16: The same d-wave function as in Fig.V.18 but for **k**=(0, 0, 2π/a), has an even smaller amplitude in the vicinity of the octahedral site than for **k**=0 as it changes sign from each atomic site to atomic site. The energy shift $\Delta E_{\mathbf{k}=(0,\,0,\,2\pi/a)}$ is consequently very small , too.

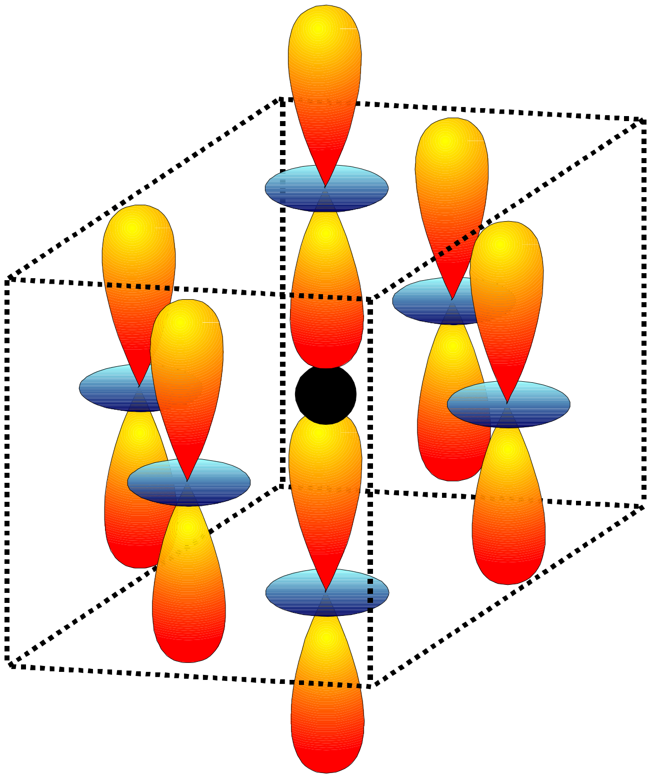

Fig. V.17: At **k**=0, the sum of the d-wave function with $3z^2$-r^2 symmetry has zero amplitude exactly at the octahedral site. The energy shift $\Delta E_{\mathbf{k}=0}$ is thus zero.

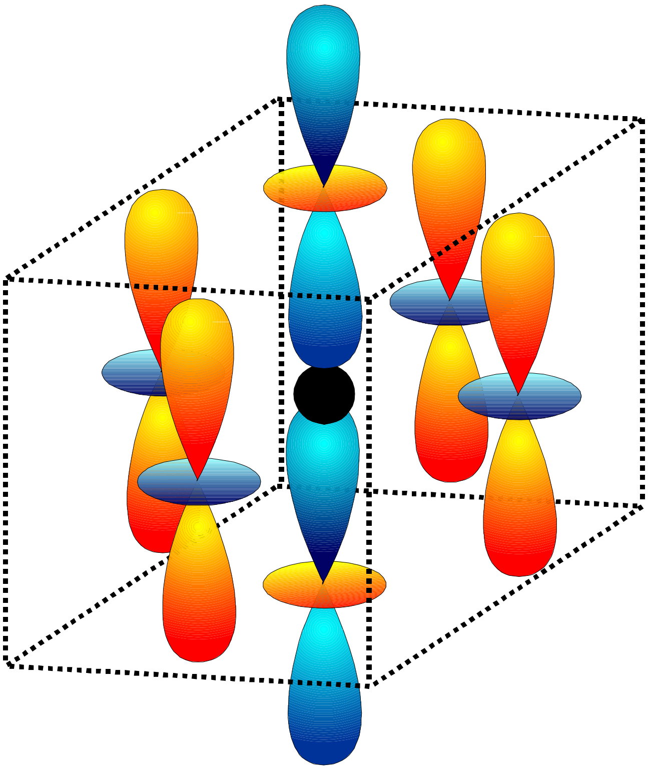

Fig. V.18: The same d-wave function as in Fig.V.20 but for **k**=(0, 0, 2π/a). There is clearly a finite overlap since all lobes of the atomic wave functions have the same sign. Therefore, the energy shift $\Delta E_{\mathbf{k}=(0,\,0,\,2\pi/a)}$ is large. For an observer sitting on the hydrogen the six d-waves create an environment with strongly s-character.

So far we have only considered special points in the Brillouin zone. For an overall impression of the influence of hydrogen on the electronic structure of a metal it is advantageous to compare the density of states of the pure metal with that of the hydride.

V.6 DENSITY OF STATES CURVES

From the E(**k**) curves it is possible to calculate the density of states function n(E) which is defined as the number of states with an energy between E and E+ dE divided by dE and, depending on the authors, furthermore divided by the number of atoms or the volume of the sample. In Fig. V.19 we show n(E) corresponding to the electronic bands given in Fig. V.1. The region of high density of states is associated with the d-bands. The Fermi energy falls just above the highest energy peak in n(E). This is the reason why the electronic properties of Pd are very sensitive to doping. The n(E) curve integrated up to E_F is equal to 10 electrons for Pd.

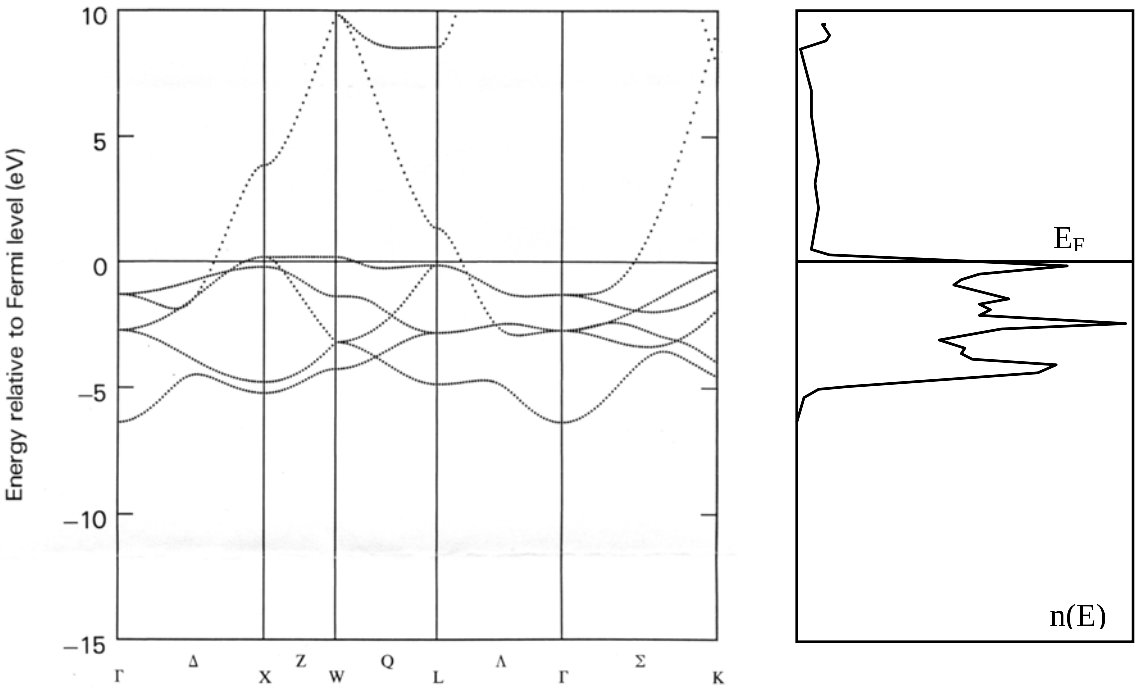

Fig. V.19: The density of states function n(E) for pure Pd. It is given in states per eV per atom.

When hydrogen is added to palladium to form PdH we have seen that the s-band is strongly lowered in energy. This produces an extra peak in n(E) at low energies as can clearly be seen in Fig. V.20. It is important to note here that this low-lying peak in the density of states does not arise because new states are created by hydrogen. It is mainly made of electronic states of the host metal which have been lowered in energy by the attractive proton potential as described in the previous section. A direct way to check that the low-lying peak does not contain new states is to look at the Fermi energy which is now clearly well above the d-bands: the extra electron introduced in the system has been used to fill up the d-band. Stoichiometric PdH is thus similar to the noble metals Cu, Ag and Au, which all have a filled d-band.

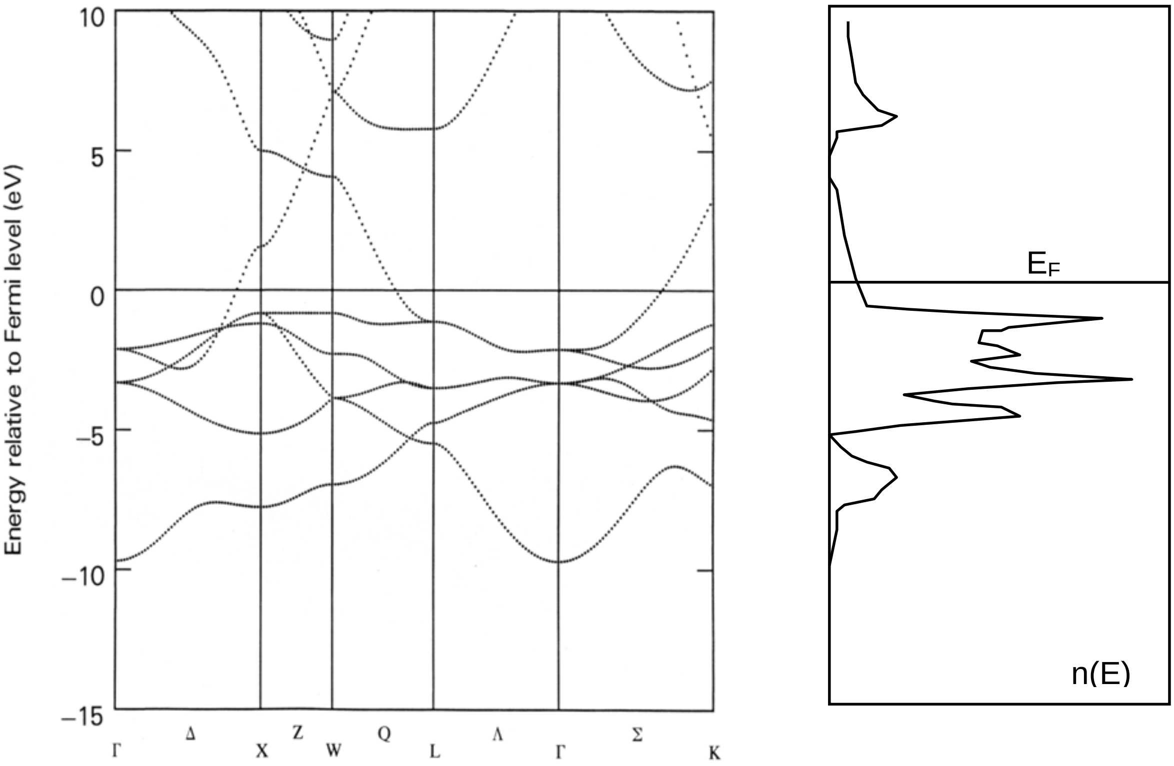

Fig. V.20: The density of states function n(E) for stoichiometric PdH. It is given in states per eV per atom.

To gain more insight in the changes induced by hydrogen in the electronic states of Pd it is useful to look at Fig. V.21 in which the density of states function has been projected onto the Pd and H sites. This is easily done in the tight-binding approximation since the atomic wave functions are by definition centred either at the Pd or the H sites. The low-lying states are strongly hybridised: there is approximately two times more spectral weight on the Pd sites than on the H site. The d-states (those which do not have a s-like symmetry at the H sites) are almost totally centred at Pd sites as expected. The contribution of the various states (s, p and d-states) at the Pd sites and at the H sites are explicitly given in Fig. V.22 and Fig. V.23, respectively. For the Pd sites we see again that the main contribution originates from the d-states which represent 89% of the Pd-density of states. At the H sites 80% of the density of states originates from the s-states. The contribution of d-states is less than 4%.

By now there is ample experimental evidence (mainly from photoemission experiments) for the existence of the low-lying band in hydrides. A very detailed study of the energy shifts induced by hydrogen in Pd has been done by Venema et al.[4] by means of the Haas-van Alphen effect. Their experiment confirms that the s-band is lowered by ~1 eV in the vicinity of the Fermi energy and that the position of the d-band remains virtually unchanged.

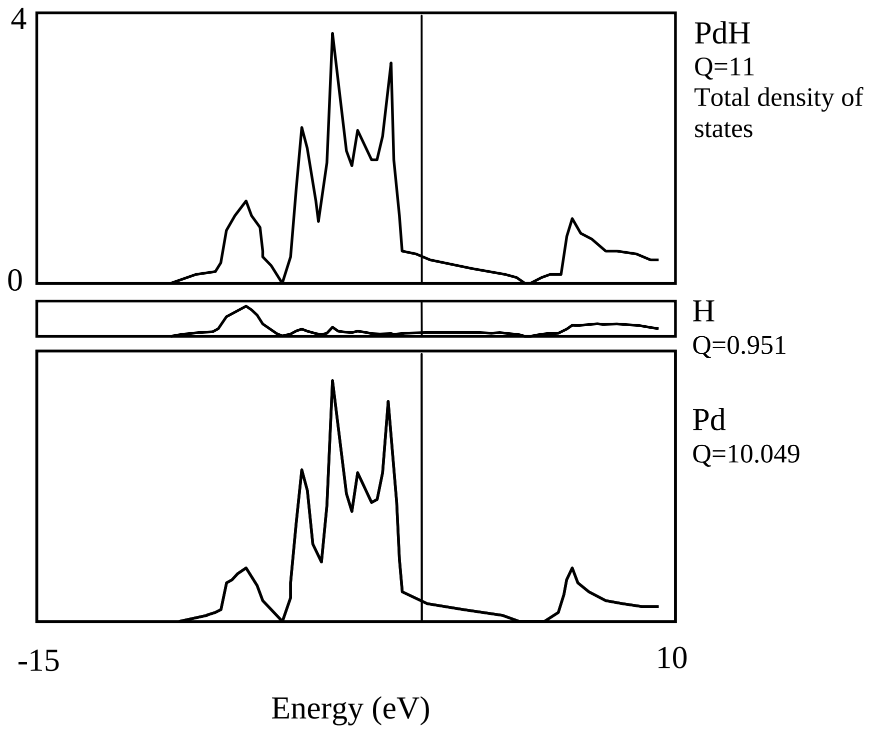

Fig. V.21: Total density of states function n(E) for PdH in units of states per eV per atom. In the middle panel we indicate the contribution of H sites and in the lower panel the contribution of Pd sites. Q gives the number of electrons (total, at H and at Pd sites).

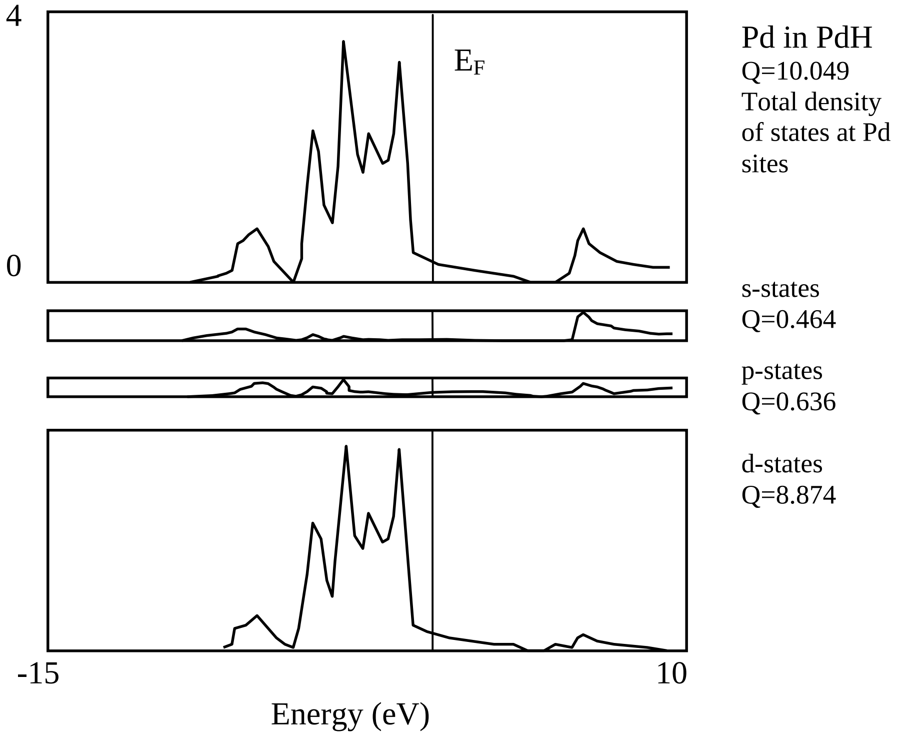

Fig. V.22:Total density of states function $n_{Pd}(E)$ of the Pd sites in PdH given in units of states per eV per atom (top panel). In the lower panels we indicate the contribution of s-, p-, and d-states at Pd sites to the total density of states. Q gives the number of electrons in Pd s-, p- and d-states.

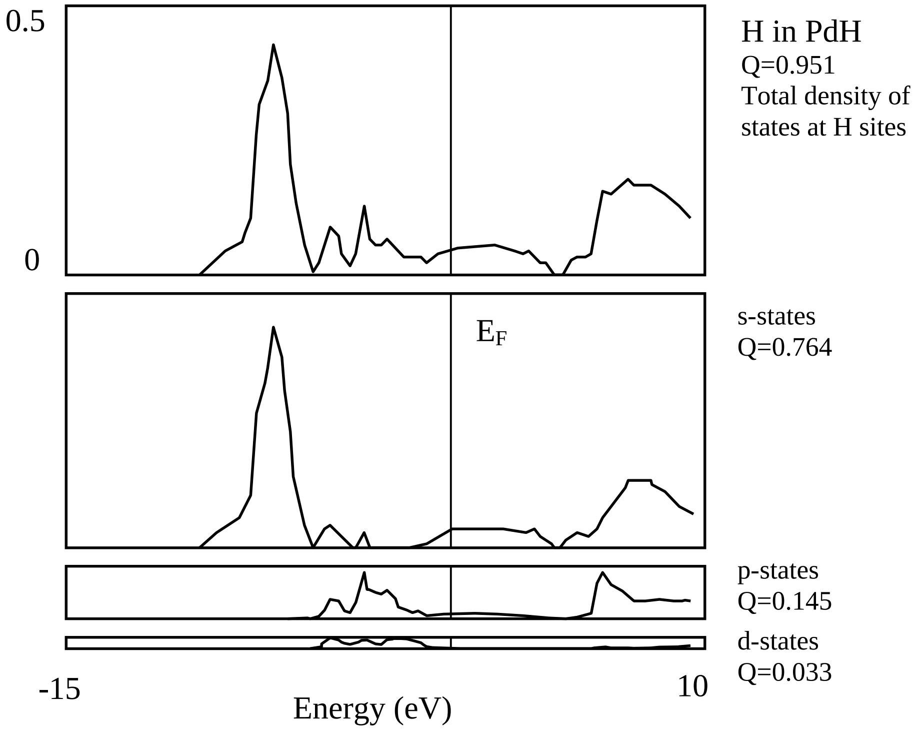

Fig. V.23: Total density of states function $n_H(E)$ of the H sites in PdH given in units of states per eV per atom (top panel). In the lower panels we indicate the contribution of s-, p-, and d-states at Pd sites to the total density of states. Q gives the number of electrons in H s-, p- and d-states.

All the features described so far for Pd and PdH are not specific for this metal-hydride system but are found in all transition metal-hydrides. A nice example, though for a hypothetical FCC YH is shown in Fig. V.24. In this case the low-lying peak in the density of states is well separated from the d-band. The case of YH is also instructive as it shows unambiguously that spectral weight has been lowered from the d-band. Two electrons are accommodated in the low-lying band and two at the bottom of the d-band. This corresponds to an effective emptying of the d-band although an extra electron is added to Y ! To illustrate this seemingly strange situation, we indicate schematically in Fig.V.28 the effect of H on the electronic structure of a transition metal having N valence electrons. The d-band of the host metal can accommodate 10 electrons. The lowest band hybridises with a s-p band and forms a band with predominantly s-symmetry at the H sites. This band contains 2 electrons. When hydrogen is added to the metal these s-like states are lowered in energy by typically 3 to 4 eV. The remaining part of the d-band, which can now accommodate only 8 electrons, is filled by N-2 electrons. In the case of Y we have N=3 and, therefore, in YH the remains of the d-band contain only 2 electrons. **This means that E_F is effectively lowered with respect to the *bottom* of the d-band although it is increasing with respect to the *top* of the d-band.** This reasoning might seem at variance with what is observed in a transition metal such as Pd where the d-band is almost full. However, in Pd we have N=9.64 and the d-band is filled up when one H is added. The Fermi energy is then pushed up into the s-p-band, which for simplicity has not been drawn in Fig.V.25. [Note that the non-integer value N=9.64 is due to the hybridisation of the d-bands with the s-p band].

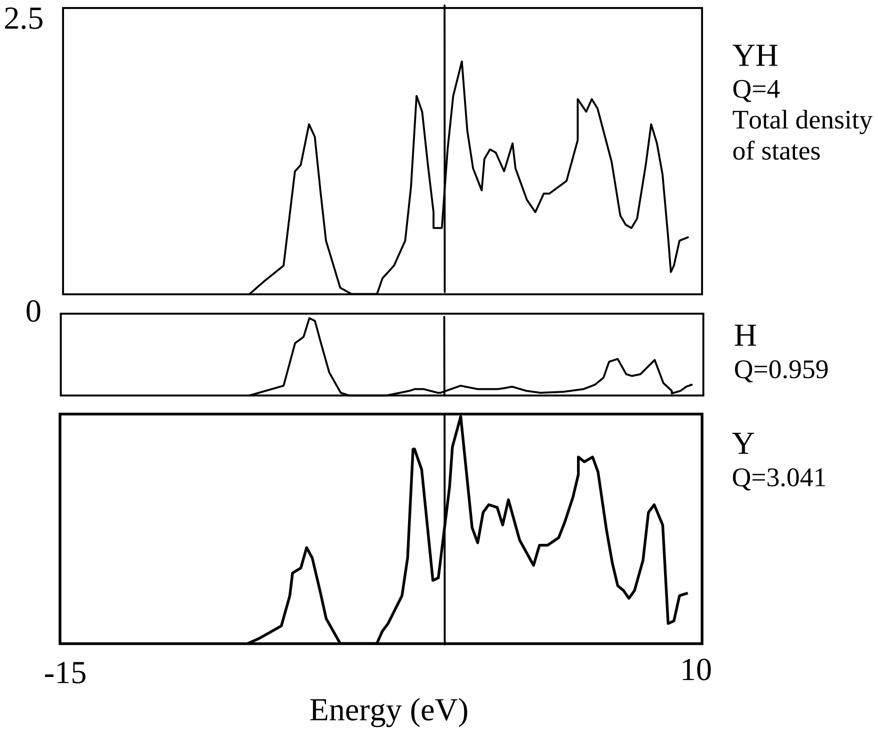

Fig. V.24: Total density of states function n(E) for YH in units of states per eV per atom. In the middle panel we indicate the contribution of the H sites and in the lower panel the contribution of Y sites. Note that the remains of the d-band contain only two electrons although the d-band contained 3 in pure Yttrium.

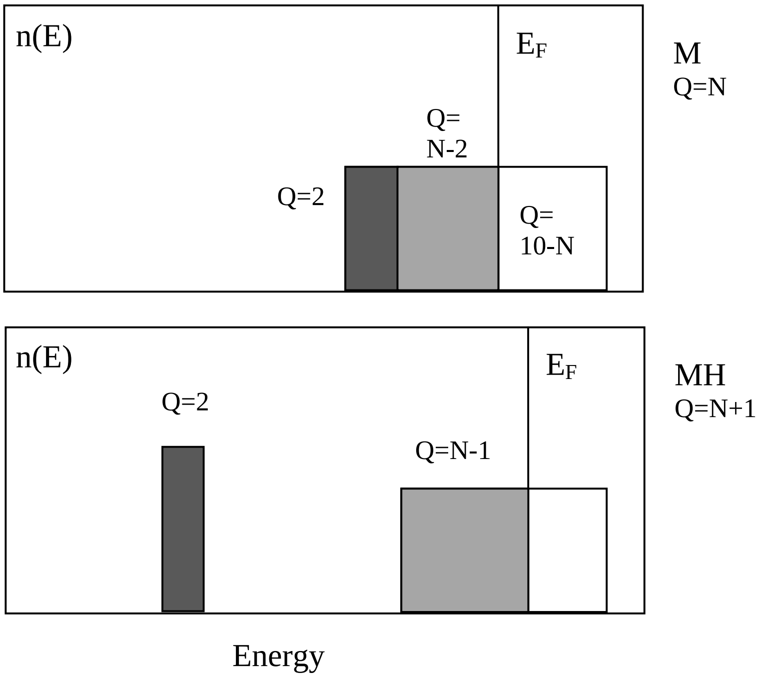

Fig.V.25: Schematic representation of the changes in the electronic structure of a metal M induced by the introduction of hydrogen in M to form a metal-hydride MH.

The influence of hydrogen on the band structure and density of states of the host metal discussed above are in fact representative for the all the transition metal monohydrides. This is clearly exhibited by recent results obtained by Smithson et al[5] for the first row of transition metal-hydrides (see Fig. V.26). In order to discuss trends the crystal structure is taken as the same rocksalt (NaCl-structure) structure for all hydrides. The peak at energies around -7 eV is mainly due to hydrogen forming a bonding state with host metal states with s-symmetry at the sites occupied by hydrogen. The red arrow indicate the position of the ground state of a free hydrogen atom measured with respect to the vacuum zero of energy indicated by the blue arrow. One would naively expect that the red arrow should always be at an energy close to –13.6 eV. However, for metals on the left of the periodic table there is an increasing tendency towards ionicity. This implies an accumulation of charges at the H sites and an increase in energy of the lowest H-band. For Sc, which has a Pauling electronegativity of 1.36 compared to 2.2 for H, the tendency towards ionic bonding is stronger than for example Ni, that has an electronegativity of 1.91.

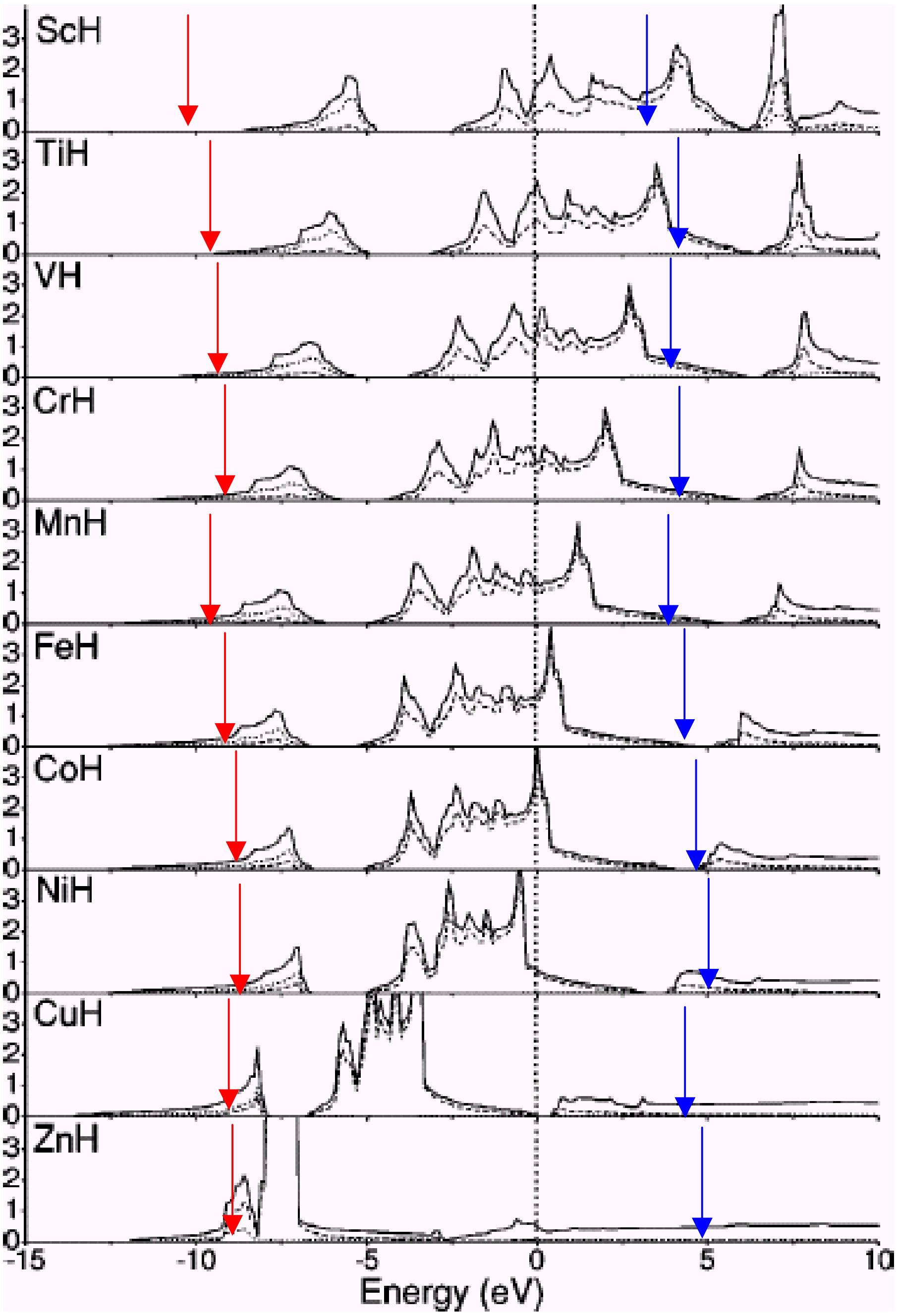

Fig. V.26: Density of states curves for the monohydrides of the 3d transition metals. The crystal structure is assumed to be the same rocksalt (NaCl-structure) structure for all hydrides. The peak at energies around 7 eV is mainly due to hydrogen forming a bonding state with host metal states with s-symmetry at the sites occupied by hydrogen. The red arrow indicate the position of the ground state of a free hydrogen atom measured with respect to the vacuum zero of energy indicated by the blue arrow. The position of the blue arrows is determined from measured values of the work function of the pure host metals.

V.7 SUB-STOICHIOMETRIC TRANSITION METAL-HYDRIDES

So far we have only considered *stoichiometric* metal-hydrides. There have been several attempts to calculate the electronic structure of non-stoichiometric alloys. One example, calculated by Gelatt et al.[6] is shown in Fig. V.27 for the case of $PdH_{0.05}$. When the hydrogen concentration increases the spectral weight of the low-lying band in PdH_x increases and is equal to 2x. At the same time the low energy hybridised s-d band loses weight and becomes fuzzy. The fuzziness is a direct consequence of the fact that the wave vector **k** is not a good quantum number in an alloy as translation symmetry has been broken. Consequently, the lifetime of these states is strongly decreased.

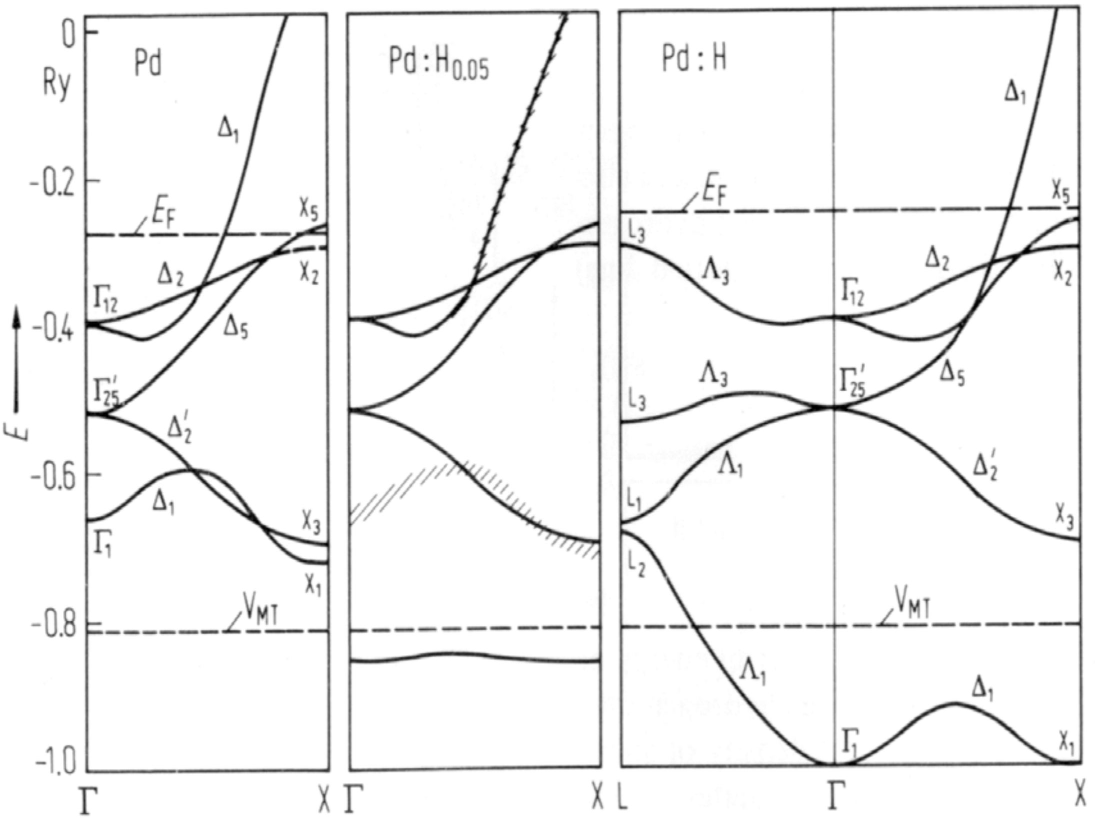

Fig. V.27: Electronic band structure of Pd, $PdH_{0.05}$ and PdH along the ΓX and ΓL directions in the Brillouin zone. The dashed regions indicate bands with states of finite lifetime (broadening due to disorder). The lower band in $PdH_{0.05}$ contains 2×0.05 electron states. These states are extracted mainly from the lowest Pd band in the left panel. With increasing x, the lower band of PdH_x broadens until stoichiometry is reached in the right panel. The zero of energy does not represent the vacuum zero since the measured work function of Pd is about 5.4 eV= 0.4 Ryd. This implies that the vacuum zero is actually at +0.11 Ryd and that the 2x band in the middle panel is really 0.96 Ryd below the vacuum level. This is essentially the ground state energy of an electron in a hydrogen atom.

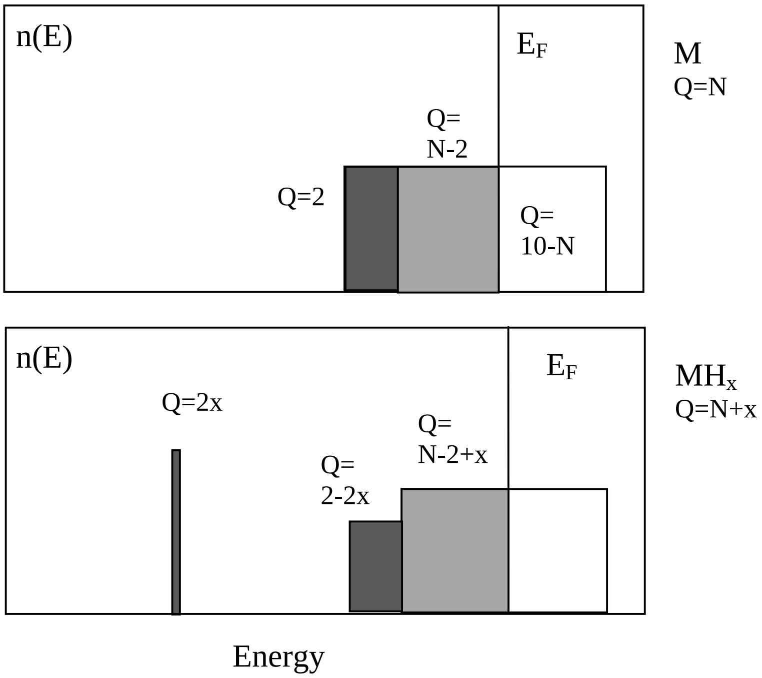

Fig.V.28: Schematic representation of the changes in the electronic structure of a metal M induced by the introduction of hydrogen in M to form a sub-stoichiometric metal-hydride MH_x.

V.8 DIHYDRIDES OF TRANSITION METALS

The density of states curves calculated by Smithson et al.[5] for the first row of transition metal-hydrides are shown in Fig. V.30. There are now two bands formed at low energies instead of only one in the monohydrides. Here again a same crystal structure (the so-called CaF_2 structure, see Fig. V.29) is assumed for all dihydrides. The formation of a double low-lying energy band can easily be understood from the following linear model. The metal atoms are on a linear chain arrangement and have two hydrogen nearest-neighbour each. One constructs first molecular orbitals for each MH_2 building block and incorporate them later into a tight-binding calculation.

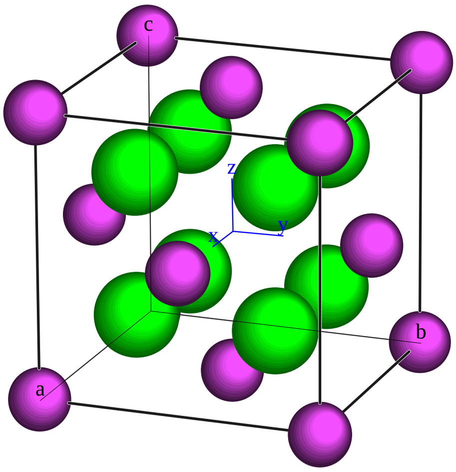

Fig. V.29: The CaF_2 structure assumed for the density of states calculations for the transition metal di-hydrides considered in Fig. V.30. Hydrogen occupies the green positions. The hydrogen atoms form a simple cubic lattice of lattice constant a/2. The metal atoms are on a FCC lattice.

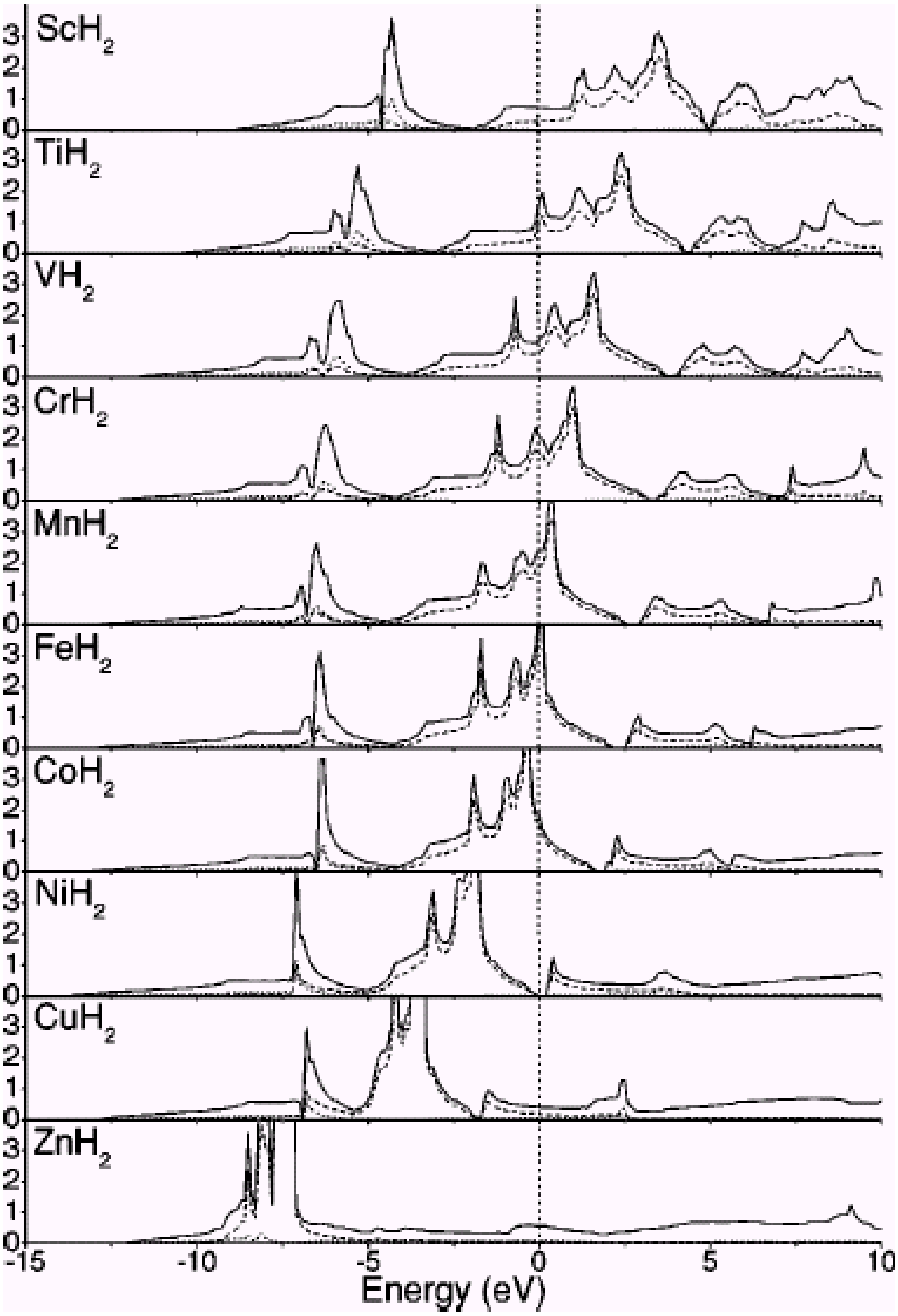

Fig. V.30: Density of states curves for the dihydride of the 3d transition metals. The double peak at energies around 7 eV is mainly due to hydrogen forming a bonding state with host metal states with s-symmetry at the sites occupied by hydrogen[5.] There is also strong hybridisation between hydrogen neighbours. This shall be discussed in the next Chapter.

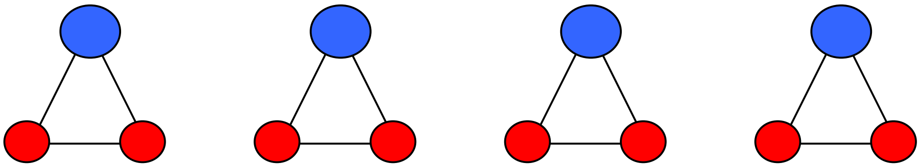

Fig. V.31: Linear model of a metal-dihydride. The blue sphere represents the metal atoms and the red one the hydrogen atoms.

In analogy with the H_2^+-molecule ion problem we introduce the following notations for simplification

$$\overline{H}_i \equiv -\frac{\hbar^2}{2m}\Delta + V(\mathbf{R}_i - \mathbf{r}) \qquad (i=M, L, R) \qquad (V.32$$

where M stands for metal, and L and R for the left and right hydrogen atoms, respectively. The atomic wave functions are for hydrogen

$$\left|L\right\rangle \equiv \phi_G\left(\mathbf{L}-\mathbf{r}\right) \qquad \left|\mathrm{R}\right\rangle \equiv \phi_G\left(\mathbf{R}-\mathbf{r}\right) \qquad (V.33$$

and for the metal (we assume in the following the it is a metal s-state)

$$\left|M\right\rangle \equiv \phi_M\left(\mathbf{R}_M-\mathbf{r}\right) \qquad (V.34$$

and correspondingly for the potentials

$$V_L \equiv V\left(\mathbf{L}-\mathbf{r}\right) \qquad V_R \equiv V\left(\mathbf{R}-\mathbf{r}\right) \qquad \text{and } V_M \equiv V\left(\mathbf{R}_M-\mathbf{r}\right) \qquad (V.35$$

We have

$$\overline{H}_L\left|L\right\rangle \equiv \left[-\frac{\hbar^2}{2m}\Delta + V_L(\mathbf{r})\right]\left|L\right\rangle = E_H\left|L\right\rangle \qquad (V.36$$

for the hydrogen atom on the left. A similar expression applies for the proton on the right. E_H is the ground state energy of the hydrogen atom. For the metal, we analogously

$$\overline{H}_M\left|M\right\rangle \equiv \left[-\frac{\hbar^2}{2m}\Delta + V_M(\mathbf{r})\right]\left|M\right\rangle = E_M\left|M\right\rangle \qquad (V.37$$

We seek a solution of the Schrödinger for one electron

$$\left[-\frac{\hbar^2}{2m}\Delta+V_M(\mathbf{r})+V_L(\mathbf{r})+V_R(\mathbf{r})\right]\Psi=E\Psi \tag{V.38}$$

as a linear combination of the atomic states $|M\rangle, |R\rangle$ and $|\mathrm{L}\rangle$, i.e.

$$\Psi=a|M\rangle+b|L\rangle+\mathrm{c}\,|R\rangle \tag{V.39}$$

Following the usual three steps indicated in chapter II we find

$$\begin{aligned}&a\left[E_M+\langle M|V_L|M\rangle+\langle M|V_R|M\rangle\right]+\\&+b\left[\langle L|\ V_L|\ M\rangle+\langle L|\ V_R|\ M\rangle\right]+\\&+c\left[\langle R|\ V_L|\ M\rangle+\langle R|\ V_R|\ M\rangle\right]=E\,a\end{aligned} \tag{V.40}$$

and

$$\begin{aligned}&a\left[\langle M|\ V_M|\ L\rangle+\langle M|\ V_R|\ L\rangle\right]+\\&+b\left[E_H+\langle L|V_M|L\rangle+\langle L|V_R|L\rangle\right]\\&+c\left[\langle R|\ V_M|\ L\rangle+\langle R|\ V_R|\ L\rangle\right]=E\,b\end{aligned} \tag{V.41}$$

nd a similar expression for the hydrogen wave function on the right. Neglecting three-center integrals for example of the form $\langle R|\ V_L|\ M\rangle$ we obtain the following matrix

$$\begin{pmatrix}E_M-2V & -t & -t\\ -t & E_H-2V & -t\\ -t & -t & E_H-2V\end{pmatrix}\begin{pmatrix}a\\b\\c\end{pmatrix}=E\begin{pmatrix}a\\b\\c\end{pmatrix} \tag{V.42}$$

in which, for simplicity, we have set

$$\langle M|\ V_M|\ L\rangle=\langle L|\ V_L|\ R\rangle=\langle R|\ V_R|\ L\rangle=-t \tag{V.43}$$

$$\langle L|V_M|L\rangle=\langle L|V_R|L\rangle=\langle R|V_M|R\rangle=\langle M|V_R|M\rangle=-V \tag{V.44}$$

although in reality the M-H and M-M tunneling matrix elements might be different from each other and similarly the Coulomb terms might differ from –V. These refinements are however irrelevant for the present qualitative discussion.

There exists a non-trivial solution if the following secular determinant vanishes

$$\begin{vmatrix} E_M - 2V - E & -t & -t \\ -t & E_H - 2V - E & -t \\ -t & -t & E_H - 2V - E \end{vmatrix} = 0 \qquad (\text{V}.45$$

There are three energy eigenvalues

$$E_1 = -2V + \frac{E_H}{2} - \frac{t}{2} + \frac{E_M}{2} - \frac{1}{2}\sqrt{(E_M - E_H)^2 + 2t(E_M - E_H) + 9t^2} \qquad (\text{V}.46$$

$$E_2 = E_H - 2V + t \qquad (\text{V}.47$$

$$E_3 = -2V + \frac{E_H}{2} - \frac{t}{2} + \frac{E_M}{2} + \frac{1}{2}\sqrt{(E_M - E_H)^2 + 2t(E_M - E_H) + 9t^2} \qquad (\text{V}.48$$

Interestingly, the eigenvector corresponding to energy E_2 is independent of the chosen parameters and has

$$a = 0, \;\; b = -\frac{1}{\sqrt{2}} \;\; \text{and} \;\; c = \frac{1}{\sqrt{2}} \qquad (\text{V}.49$$

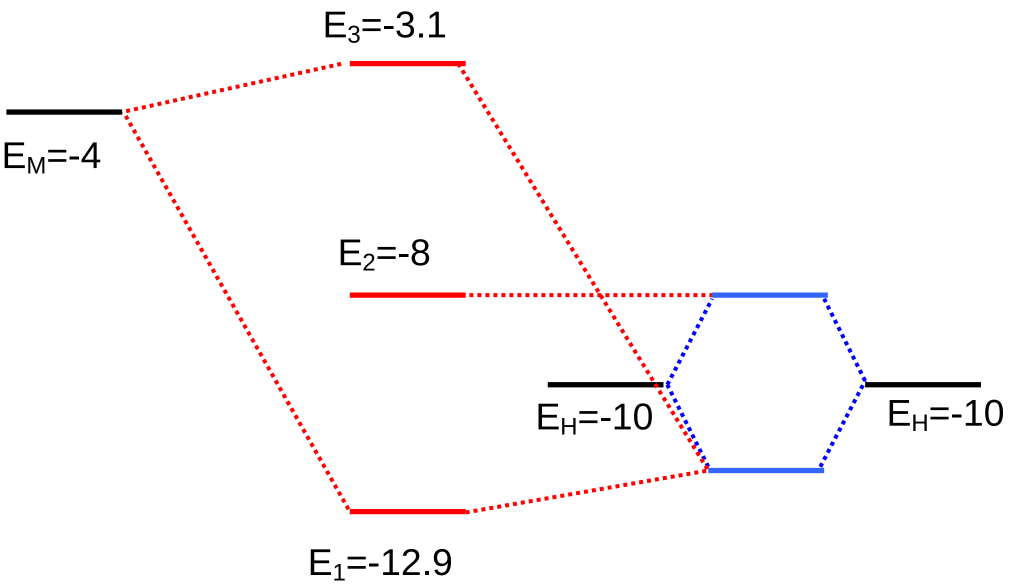

Fig. V.32: Energy eigenvalues of the MH_2 building block shown in Fig. V.31 for a hypothetical case in which E_H=-10 eV, E_M=-4 eV, V=0 and t=2 eV. For clarity we have shown how the two atomic H-wave functions are first forming a bonding and an antibonding state. The bonding state hybridizes then with the metal atomic wave function to form a new set of bonding and antibonding states. The antibonding state of the H_2 molecule does not couple to the metal wave function. This is due to the chosen symmetric arrangement of the H atoms with respect to the metal atom. This is reasonable since it is also the case in the CaF_2 structure.

i.e. this state corresponds to the antibonding state of the H_2 molecule in absence of electro-electron interaction. It has zero admixture of the metal atomic wave function. The other two states involve linear combination of all three atomic states. In Fig. V.33 we give a numerical example for the case of E_H=-10 eV, E_M=-4 eV, V=0 and t=2 eV.

The energy eigenvalues are (with the corresponding eigenvectors given in parentheses),

E_1=-12.9 eV (0.30, 0.67, 0.67) (V.50

E_2=-8.0 eV (0, -0.707, 0.707) (V.51

and

E_2=-3.1 eV (0.95, -0.21, -0.21) (V.52

The eigenstates are illustrated in Fig. V.33. The two lower states have predominantly a H-character and correspond to the two low-lying bands in Fig. V.30. The upper state has predominantly metallic character and corresponds to the host metal bands. To be complete one

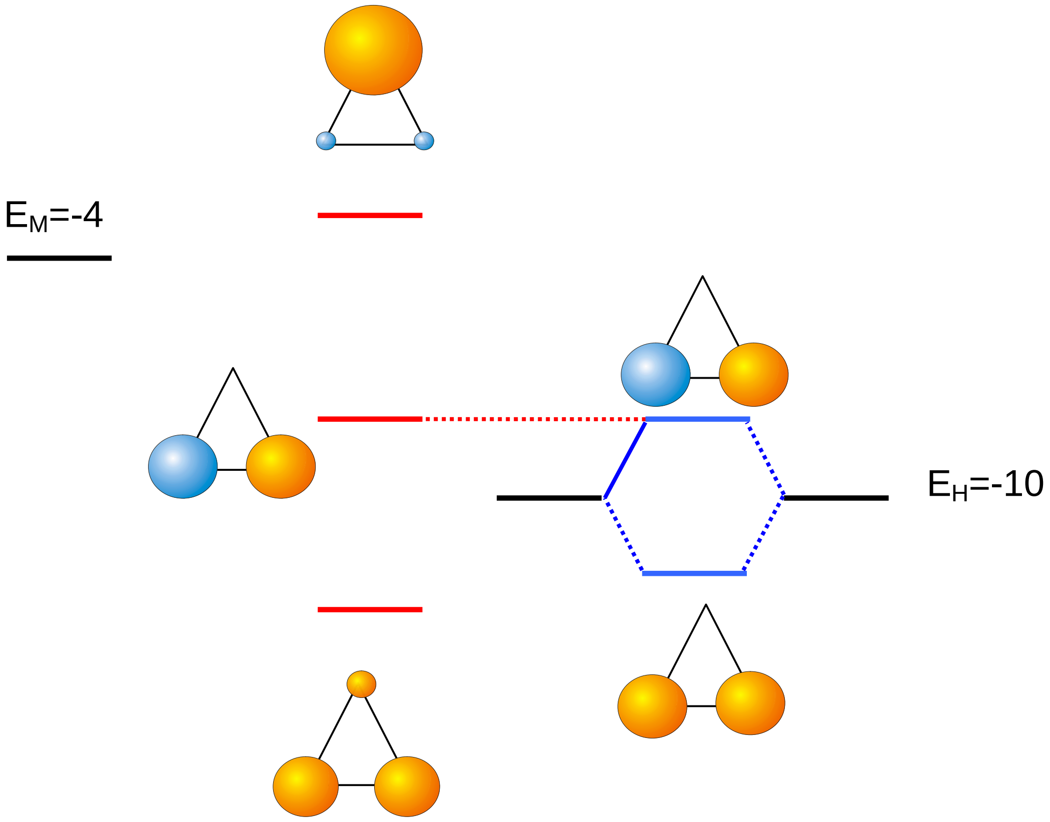

Fig. V.33: Schematic indication of the eigenstates corresponding to the energy eigenvalues of the MH_2 building block given in Fig. V.32. Orange corresponds to a positive sign of the wave function and blue to a negative sign. The diameter of the spheres is taken proportional to the coefficients a, b and c in Eq.V.39.

should now discuss the influence of the d-states. We will postpone this discussion to Chapter VI when we consider the electronic structure of Y and La dihydrides and trihydrides.

V.9 REFERENCES

---

[1] Moruzzi, V. L. (1984) : we are greatly indebted to V. L. Moruzzi for making available band structure calculations of many interstitial compounds.

[2] Fermi surface web page: http://www.phys.ufl.edu/fermisurface/index.html

[3] Slater, J.C., and G. F. Koster, Phys. Rev. **94** (1954) 1498

[4] Venema, W. J., PhD thesis (1980); see also Bakker, H. L. M., R. Feenstra, R. Griessen, L. M. Huisman and W. J. Venema, Phys. Rev. **B26** (1982) 5321

[5] Smithson, H., C.A. Marianetti, D. Morgan, A. van der Ven, A. Predith and G. Ceder, Phys. Rev. B66 (2002) 144107

[6] Gelatt, C.D., H. Ehrenreich, J. A. Weiss, Phys. Rev. **B 17** (1978)1940